IL-17-producing CD8$^+$ T cells promote PDAC via induction of inflammatory cancer-associated fibroblasts

Felix S.R. Picard[1*], Veronika Lutz[1*], Anna Brichkina[2*], Felix Neuhaus[1], Teresa Ruckenbrod[1], Anna Hupfer[2], Hartmann Raifer[1,3], Matthias Klein[4], Tobias Bopp[4], Petra I. Pfefferle[5], Rajkumar Savai[6,7], Immo Prinz[8], Ari Waisman[9], Sonja Moos[9], Hyun-Dong Chang[10,11], Stefan Heinrich[12], Detlef K. Bartsch[13], Malte Buchholz[2], Shiv K. Singh[14], Mengyu Tu[14], Lukas Klein[14], Christian Bauer[2], Robert Liefke[15,16], Andreas Burchert[16], Ho-Ryun Chung[17], Philipp Mayer[18], Thomas M. Gress[2], Matthias Lauth[2], Matthias M. Gaida[19-21], Magdalena Huber[1]

Supplementary Information

1. **Supplementary Methods and References**
2. **Supplementary Tables 1-6**
3. **Supplementary Figures 1-10**

1. Supplementary Methods and References

Human and Murine Tissue sample histology

For histological analysis, human PDAC tumor tissue samples were provided by the tissue bank of the University Medical Center Mainz in accordance with the regulations of the tissue biobank and the approval of the ethics committee of University Medical Center Mainz (2019-14390; Landesärztekammer RLP). Tissue samples of 112 (supplementary table 1) patients with therapy naive pancreatic ductal adenocarcinoma (PDAC), who underwent surgical resection, were spotted on microarrays to obtain paraffin tissue sections for further analysis. To overcome heterogeneity, 4 array spots of each tissue were generated (2 central, 2 peripheral; diameter: 1 mm).

Murine tissue samples were taken from tumors and healthy pancreatic tissue of KPC mice, and from Panc^{OVA}-induced subcutaneous tumors, and then embedded in paraffin.

After deparaffinization, rehydration, and antigen retrieval in pH 6 (human triple and double staining) or pH 9 (murine triple staining) conditions, the following antibodies were used for human triple staining: anti-human(h)IL-17A (Biotechne, MAB3171), anti-hCD8 (DAKO, GA62361-2), and anti-hαSMA (DAKO, GA61161-2). For human double staining following antibodies were applied: anti-hCD8 (DAKO, GA62361-2), and anti-hRORγt (Biozol, LS-

Picard FSR, *et al. Gut* 2023; 72:1–13. doi: 10.1136/gutjnl-2022-327855

B4659-100) or anti-hCD4 (Agilent, IR649). DAKO Envision Flex system (brown) and permanent Green (Zytomed) were used for visualization. For human CK5 and GATA6 double staining following antibodies were applied: anti-hCK5 (Leica, CK5-L-CE), anti-hGATA6 (Biotechne, AF1700). DAKO Envision Flex system (brown) and permanent Magenta Chromogen (red) were used for visualization. For murine triple staining following antibodies were applied: anti-mouse(m)IL17A (abcam, ab91649), anti-mCD8 (LSBio, LS-C414175), anti-mαSMA (Cell Signalling, #19245). For the signal amplification of primary antibodies, EnVision FLEX+ Mouse and Rabbit (LINKER) were used (#K8002, #K8009, Agilent, DAKO). DAKO Envision Flex system (brown), permanent Magenta Chromogen (red) and permanent Green (Zytomed) were used for visualization. $CD8^+IL\text{-}17A^+$, $CD8^+ROR\gamma t^+$, $CD4^+RORgt^+$, total $CD8^+$, total $IL\text{-}17A^+$ cells were counted per mm^2. The amounts of $CK5^+$ or $GATA6^+$ tumor cells are expressed as percent of total tumor cells as previously described.[1] Images were taken using the Gryphax Subra camera (Jenoptik, Jena, Germany). For confirmation of results, quantification was done using the ImageJ software.

For Masson-Goldner trichrome staining, paraffin tissues were deparaffinized in xylene and re-hydrated with graded alcohols. Standard staining procedure was performed using hematoxylin, followed by staining with Mallory Red, Phosphomolybdic Acid (1%), light green, and acidic acid (all chemicals provided by Merck, Darmstadt, Germany). Slides were dehydrated in 100% ethanol and xylene and mounted for further microscopy.

Isolation, Stimulation and staining of human TILs from PDAC patients

For FACS analysis, human PDAC tumor and healthy tissues were collected by the CBBMR (Comprehensive Biomaterials Bank Marburg). Tumor and control tissues were digested by 200 U ml^{-1} Collagenase IV (Worthington), 10 µg ml^{-1} DNAse 1(Roche) in HBSS, 37°C, 300 rpm agitation and filtered through 100 µm cell strainers (Sysmex). Single cell suspensions were restimulated for 5 h with PMA (50 ng ml^{-1}), Ionomycin (1 µg ml^{-1}, both from Sigma-Aldrich), after 3 h in the presence of brefeldin A (5 µg ml^{-1}; BioLegend). The cells were stained with: Zombie NIR fixable viability kit (Zombie NIR™ Fixable Viability Kit, BioLegend # 423106), anti-hCD3 (AF488, BioLegend #317310), anti-hCD4 (PacificBlue, BioLegend #300521) and anti-hCD8 (BV510, BioLegend #344732) for 45 min at 4°C. After fixation (2% *para*-formaldehyde 20 min, 4°C), intracellular staining in Saponin Buffer (0.1% Saponin, 1% BSA in PBS) was done for hIL-17A (PE #512306 BioLegend) and hIFNγ (APC, #502512

Picard FSR, *et al. Gut* 2023; 72:1–13. doi: 10.1136/gutjnl-2022-327855

BioLegend) for 45 min at 4°C. Samples were measured and analyzed on an FACS Aria III (BD Biosciences), with FACS Diva and FlowJo V10.1.

Patient involvement

Tissue samples of 112 (supplementary table 1) patients with therapy naive pancreatic ductal adenocarcinoma (PDAC), who underwent surgical resection, were provided by the tissue bank of the University Medical Center Mainz in accordance with the regulations of the tissue biobank and the approval of the ethics committee of University Medical Center Mainz (2019-14390; Landesärztekammer RLP).

Mice

WT C57BL/6 CD45.2^{+}CD45.1^{-}, congenic C57BL/6 CD45.2^{-}CD45.1^{+} mice were bred in-house (Animal Facility Philipps-University Marburg, BMFZ). *Rag1*$^{-/-}$ (B6.129S7-Rag1tm1Mom/J) mice were received from Dr. H.D. Chang, TU Berlin, Germany. OT-I (B6.Cg-Tg(TcraTcrb)1100Mjb) mice were obtained from Jackson Laboratories. To obtain KPC mice, *LSL-Kras*$^{G12D/+}$*LSL-Trp53*$^{R172H/+}$ were crossed with *Pdx-1-Cre* mice to yield triple-mutant mice *LSL-Kras*$^{G12D/+}$*LSL-Trp53*$^{R172H/+}$*Pdx-1-Cre*, the F1 was genotyped by PCR. KPC^{+} animals underwent weekly palpation and ultrasound screening starting from week 10. IL-17A/F DKO (B6.Cg-Il17a/Il17ftm1.1Impr Thy1a/J) mice were received from Dr. I. Prinz, UKE Hamburg, Germany. *Il17ra* $^{-/-}$ (IL-17ra$^{tm1.2Kurs}$)[2] mice were received from Dr. R. Savai, Max Planck Institute, Bad Nauheim, Germany, and Dr. A. Waismann, Johannes Gutenberg University Medical Center, Mainz, Germany. Athymic nude mice (athym-*Fox1*$^{nu/nu}$), which are T-cell- but not NK-cell-deficient, and C57BL/6J mice for orthotopic tumor transplantation were obtained from Janvier Labs. All studies were approved by the regional agency on animal experimentation (Regierungspräsidium Giessen).

Murine T cell purification and *in vitro* differentiation

CD8^{+} T cells were obtained from lymph nodes (LNs) and spleens of WT or IL-17A/FDKO C57BL/6 mice (for all CM production or for adoptive transfer experiments depicted in figure 6), or of OT-I mice (for adoptive transfer depicted in figure 2A,C) using a negative selection kit (130-104-075, Miltenyi Biotec). For Tc17 differentiation, naïve CD8^{+} T cells were cultured in RPMI (10% FCS) and stimulated with plate-bound anti-mCD3 mAb (5 µg ml^{-1}, clone 145-2C11, Biolegend) and soluble anti-mCD28 (0.5 µg ml^{-1}, clone 37.51, Biolegend) in the presence of rhIL-2 (50 U ml^{-1}, Novartis), rhTGF-β (0.5 ng ml^{-1}, Peprotech) rmIL-6 (30 ng ml^{-1},

Peprotech) and anti-mIFNγ (5 µg ml^{-1}, clone XMG1.2, Biolegend). CTL skewing conditions were achieved in RPMI (10% FCS) with plate-bound anti-mCD3 mAb (3 µg ml^{-1}) and soluble anti-mCD28 (0.5 µg ml^{-1}), rhIL-2 (50 Uml^{-1}), rmIL-12 (10 ng/ml^{-1}, Peprotech) and anti-mIFNγ (5 µg ml^{-1}). For intracellular cytokine staining, cells were restimulated after 72h of culture with PMA (50 ng ml^{-1}), Ionomycin (1 µg ml^{-1}, both from Sigma-Aldrich) in the presence of Brefeldin A (5 µg ml^{-1}; Biolegend) for 4h. After live/dead staining (Zombie NIR™ Fixable Viability Kit (# 423106 BioLegend), surface staining for CD8 molecule expression (anti-mCD8α FITC #11008182 BD Bioscience) was done for 20 min in cold PBS+1% FCS at 4°C, prior to fixation with 2% *para*-formaldehyde for 20 min at room temperature (RT). After fixation, intracellular staining in Saponin Buffer (0.1% Saponin, 1% BSA in PBS) was done for IL-17A (PE #12-7177-81 eBioscience or APC #17-7177-81 eBioscience) IL-17F (PE, #12-7471 eBioscience) and IFNγ (PerCp-Cy5.5, #505822 BioLegend) for 45 min at 4°C. Staining of transcription factors was performed without restimulation using the FOXP3/Fixation-Kit (eBioscience, 00-5521-00). For intranuclear staining, anti-m/hT-bet (eFluor660 #50582582 eBioscience) and anti-mRORγt (PE #12-6981-82 eBioscience) antibodies were diluted in 0.1% Saponin in PBS. The cells were acquired on the Attune NxT Cytometer (Thermofisher Scientific).

Conditioned Media (CM) production

For CM production, *in vitro* differentiated CTLs, Tc17 or Tc17-DKO cells generated from purified $CD8^+$ T cells obtained from spleens and LN of WT or IL-17A/FDKO C57BL/6 mice were harvested, washed with PBS, re-seeded in 24 well-plate 1×10^6 cells in 1 ml fresh DMEM (2% FCS) and restimulated with plate-bound anti-CD3 mAb (5µg ml^{-1}). Supernatants were harvested after 24h of restimulation, then centrifugated at 400× *g*, 10 min, 4°C and stored at -80°C for further use. CM from fibroblast were harvested after 48h of skewing with medium or respective CM obtained from WT or IL-17A/FDKO Tc17 cells or with TGFβ.

Bead assay

Cytokine levels from cell-culture supernatants were assessed by LEGENDPLEX MU Th17 v2 (#740749 741048 Biolegend) according to manufacturer's protocol.

Generation of stable $Panc^{OVA/Luc}$ and KPC^{luc} cells

$Panc^{OVA}$ cells[3] and KPC cells were transfected (Trans-IT-2020 (Mirus Bio)) with a firefly luciferase-expressing construct (PGK-Luc) and with an empty pEF6/V5-His plasmid (=EF-

MCS; Invitrogen) to confer Blasticidin resistance (ratio 9:1). Subsequently, cells were selected with Blasticidin (5µg ml^{-1}) and pooled, resistant clones were used in the experiments.

Culture of human and murine pancreatic tumor cell lines

Adherent PaTu8988T[4], $Panc^{OVA}$ (derived from Panc02), $Panc^{OVA/Luc}$ and pancreatic adenocarcinoma cells derived from a spontaneous KPC mouse tumor (termed KPC tumor cells), KPC^{Luc} cells were grown in T75 flasks (Sarstedt) with DMEM (10% FCS) and split every 2-4 days upon reaching 70% confluence, harvested by trypsinization (1x Trypsin/EDTA, Sigma T-4174) and reseeded (5 x 10^5 cells / 20 ml Medium / T75 flask)

Cell titer assays

Pancreatic cancer organoids (human: from PDAC patient; mouse: from KPC model[5] were established according to Boj et al[6] and treated with rhIL-17 (IL-17A, 50 ng ml^{-1}, Miltenyi Biotec, #130-093959) for 5d in organoid medium. Subsequently, cell titers were measured using the Cell Titer 3D GLO kit (Promega) (figure 2G).

$Panc^{OVA/Luc}$ or KPC^{Luc} cells (figure 2F) were seeded at 1×10^4 cells per well in 24-well TC-plate (Sarstedt) and starved for 24h with FCS-free DMEM. After 24h the medium was exchanged and tumor cells were cultured alone in DMEM 0% FCS (control) or in DMEM 2% FCS, or in DMEM 2% FCS containing IL-17A (50 ng ml^{-1}), Tc17-CM (20%) or Tc17 cells (1×10^3) per well. After 36h cells were washed with PBS and lysed in 100 µl of lysis buffer. Firefly luciferase activity was measured in 10µl lysate with 50µl luciferase solution (Beetle-Juice Luciferase assay Firefly, P.J.K.Biotech #102511) using OrionL luminometer (Berthold detection systems).

Co-cultures of primed PSC and $Panc^{OVA/Luc}$ cells (figure3J) were set up by harvesting single matrigel droplets of TGFβ-myCAF, IL-17A-iCAF, Tc17-iCAF or DKO-CAF, removing the matrigel by incubation with ice-cold DMEM and centrifugation (1000 rpm, 4°C, 5 min), and removing the supernatant. $Panc^{OVA/Luc}$ (2×10^5) cells alone or with TGFβ-myCAF, IL-17A-iCAF, Tc17-iCAF or DKO-CAF (4×10^5) were re-seeded in 70 µl in fresh matrigel and mixed at a 1:1 ratio with DMEM (10% FCS) on a 3.5 cm suspension dish (Sarstedt). The matrigel-embedded PSC and $Panc^{OVA/Luc}$ cells were covered with 0.5% FCS-containing DMEM. After 36h cells were washed with PBS and lysed in 100µl of lysis buffer. Firefly luciferase activity was measured in 10µl lysate with 50µl luciferase solution (Beetle-Juice Luciferase assay Firefly, P.J.K.Biotech #102511) using OrionL luminometer (Berthold detection systems).

Culture and priming of human and murine pancreatic stellate cells (PSC)

Pancreatic stellate cells (mPSC4[7], kindly obtained from Dr. A Neese and hPSC[8], kindly obtained from Dr. M Löhr) were cultured in T75 flasks or TC-treated dishes (Sarstedt) in DMEM (10% FCS) and split every 4-7 days, upon reaching 70% confluence. They were harvested by trypsinization (1x Trypsin/EDTA, Sigma T-4174) and reseeded (2.5×10^4 cells/ml). To obtain quiescent (q)PSC, 6×10^5 PSC were seeded in a 70 µl matrigel drop (Growth Factor Reduced (GFR) Basement Membrane Matrix, Corning, 356230) and mixed at a 1:1 ratio with DMEM (10% FCS) on a 3.5 cm suspension dish (Sarstedt). The matrigel-embedded PSC were covered with 0.5% FCS-containing DMEM and incubated for 48h. Thereafter, the medium was removed. qPSC were treated in 0.5% FCS-containing DMEM with either rhTGFβ1 (2 ng ml^{-1}; Peprotech, #100-21), rmIL-17A (50 ng ml^{-1}; Peprotech, #210-17), rhIL-17A (50 ng ml^{-1}; Peprotech, #200-17), rmIL-17F (50 ng ml^{-1}; Peprotech, #210-17F), rhIL-17F (50 ng ml^{-1}; Peprotech, #200-25), rhTNF (5 ng ml^{-1}; Peprotech, #300-01A-10), rmαTNF (5 µg ml^{-1}; ImmunTools, #12343014), rmIFNγ (50 ng ml^{-1}; ImmunTools, #12343536), rhIL-1α (5 ng ml^{-1}; Peprotech, #200-01A) or in 30% conditioned media (CM) as in each experiment indicated. After 48 h of differentiation, qPCR-based phenotyping was performed. For this, medium was removed and drops were collected in eppendorf tubes mixed with ice cold PBS. After centrifugation (1000 rpm, 4°C, 5 min) and removing of PBS, cells were resuspended in ice cold PBS and incubated for 30 min at 4°C. Cells were centrifuged (1000 rpm, 4°C, 5 min), and pellets were frozen at -80°C for later RNA preparation.

PSC transfection with CD90.1 marker

MSCV-IRES-Thy1.1 DEST vector (Addgene #17442) viral supernatants were generated from Phoenix cells and used for polybrene (8 µg/ml) assisted spin-infection according to Campos et al[9]. Resting mPSC4 at ~65% density was used as recipient cells, grown for 72 h post-spin-infection and sorted for CD90.1 expression after surface staining (anti-CD90.1 BV510, BioLegend # 202535). Surface marker expression stability was assessed by subsequent CD90.1 staining and FACS analysis, when cell cultures were split or re-thawed.

IL-17RA CRISPR/Cas9 knockout in mPSC

To knockout IL-17RA in PSC LentiCRISPRv2 (Addgene no. 52961) constructs were used. Mouse PSC were transfected with a single guide (sg)RNA targeting *mIl17ra* (CAGAAGCAGCCATCCCAGCG) using Opti-MEM (Thermo Fisher Scientific; 31985062) and polyethylenemine (PolyScience; 23966). After selection with 10 µg ml^{-1} blasticidin (Gibco;

R21001) single cells were picked and plated as single clones in 96-well plates. Knockout was verified via FACS and WB. For FACS staining PSC were harvested, matrigel dissolved by incubation with Collagenase D (5 mg ml^{-1}, Roche) and DNase 1 (10 µg ml^{-1}, Roche) in HBSS at 37°C for 5-8 min. The cells were washed with PBS and Live/Dead staining performed (Zombie NIR™ Fixable Viability Kit, BioLegend # 423106). After washing with PBS/1%FCS and centrifugation (400xg, 4°C, 5 min) surface staining for Ly6c expression (anti-mLy6c BV421 #48593182 eBioscience) was done for 20 min in cold PBS+1%FCS at 4°C, prior to fixation with 2% *para*-formaldehyde. Then intracellular receptor staining in Saponin Buffer was done for IL-17RA (PE #12-7182-82 eBioscience) and IL-17RC (APC #FAB2270A R&D Systems) for 45 min on ice. Following matching isotype controls were used: Goat IgG Isotype Control (#403006 BioLegend) and Rat IgG2a, κ Isotype Control (#554689 BD Biosciences). For human fibroblasts the receptor staining was performed as described above with the following antibodies: anti-hIL-17RA PE (#FAB177P R&D Systems), anti-hIL-17RC APC (#FAB22691A R&D Systems), Mouse IgG1 κ Iso Control PE (#12-4714-42 eBiosciences) and Mouse IgG2b κ Iso Control (#555745 BD Pharmingen).

Western Blotting

Whole cell lysates were generated using RIPA buffer. Protein concentration was measured via Lowry assay. Proteins were electrophoresed, after boiling, on 6% sodium dodecyl sulfate polyacrylamide gel electrophoresis (SDS-PAGE) gel and blotted on PVDF membrane. After blocking with 5% milk powder for 1 h, membranes were incubated with primary antibodies over night at 4 °C (anti-IL-17RA R&D Systems AF488, 1:1000; anti-Tubulin Sigma-Aldrich MAB3408, 1:10000). Membranes were washed 3 times for 10 min with TBST and incubated 1h with respective secondary antibodies (anti-goat-HRP Santa Cruz sc2020, 1:1000; anti-mouse GE healthcare NA931V, 1:20000). After three washing steps with TBST proteins were visualized in a ChemiDoc system (BioRad) after incubation with a chemiluminescence detection reagent (Santa Cruz sc2048; Thermo Fisher 34095).

Tumor cell and CAF co-cultures

For co-culture and subsequent sorting, murine $qPSC^{CD90.1}$ were primed for either Tc17-iCAF, TGFβ-myCAF or qPSC control condition as described above. $Panc^{OVA}$ cells were harvested from adherent cell cultures, counted, and stained with Cell Proliferation Dye eFluor 670 (#65-0840-90 eBioscience) according to manufacturer's protocol.

Co-cultures of primed PSC and labelled Panc^{OVA} cells (figure 5) were set up by harvesting single matrigel droplets of qPSC, Tc17-iCAF or TGFβ-myCAF, removing the matrigel by incubation with ice-cold DMEM and centrifugation (1000 rpm, 4°C, 5 min), and removing the supernatant. Labeled Panc^{OVA} (2.5×10^5) cells and qPSC, Tc17-iCAF or TGFβ-myCAF (3.5×10^5) were re-seeded in 70 µl of fresh matrigel and mixed at a 1:1 ratio with DMEM (10% FCS) on a 3.5 cm suspension dish (Sarstedt). The matrigel-embedded PSC were covered with 0.5% FCS-containing DMEM.

Co-cultures of iCAF, Tc17 cells and labelled Panc^{OVA} cells (supplementary figure 8) were set up by harvesting single matrigel droplets of Tc17-iCAF followed by removing the media and the matrigel by incubation with ice-cold DMEM and centrifugation (1000 rpm, 4°C, 5 min). Labeled Panc^{OVA} (2.5×10^5) cells alone, mixed with Tc17-iCAF (3.5×10^5) or mixed with (2.5×10^4) differentiated Tc17 cells were re-seeded in 70 µl of fresh matrigel and mixed at a 1:1 ratio with DMEM (10 % FCS) on a 3.5 cm suspension dish (Sarstedt). The matrigel-embedded PSC were covered with 0.5 % FCS-containing DMEM.

After 48h, the matrigel droplets were harvested, dissolved by incubation with Collagenase D (5 mg/ml, Roche) and DNAse 1 (10 µg/ml, Roche) in HBSS at 37°C for 45 min. The cells washed twice with cold MACS buffer (2% FCS, 1 mM EDTA in PBS), centrifuged (400x *g* ,4°C, 5 min), resuspended in MACS buffer, stained with CD90.1 antibody (BV510, BioLegend # 202535) and sorted into eFluor670$^+$ fractions on a FACS ARIA II. The eFluor670$^-$ CD90.1$^+$ fibroblast population was subsequently stained and phenotype was analyzed by FACS on an Attune Nxt (ThermoFisher). The eFluor670$^+$ tumor cell fraction was resuspended in RLTplus buffer (Qiagen) and snap-frozen for RNA isolation and RNAseq.

cDNA synthesis and qPCR analysis

RNA was isolated from *in vitro* cultured fibroblasts with the NucleoSpin RNA kit (Macherey-Nagel) or from FACS-sorted murine fibroblasts and/or tumor cells with RNeasy Plus kit (Quiagen) according to manufacturer's protocol. For cDNA synthesis, the RevertAid first strand cDNA synthesis kit (ThermoFisher Scientific) was used according to manufacturer's protocol. For qPCR analysis of Fibroblast marker genes, iTaq Universal SYBR Green (BioRad) on a StepOne (ThermoFisher Scientific) was used, with primers optimized for the standard qPCR reaction setup.

qPCR Primers

mSaa1/2	CATGCTCGGGGGAACTATGATGCTG	CTGTTGGCTTCCTGGTCAGCAATGG
mSaa3	CATGCTCGGGGGAACTATGATGCTG	AAGTGGTTGGGGTCTTTGCCACTCC
mCxcl1	GAGGCTTGCCTTGACCCTGAAGCTC	GTCAGAAGCCAGCGTTCACCAGACA
mIl6	TCCTTCCTACCCCAATTTCCAATGCTC	GGATGGTCTTGGTCCTTAGCCACTCCT
mCsf3	TGGACTTGCTTCAGCTGGATGTTGC	AGGCAGAAGTGAAGGCTGGCATGG
mCol4a1	TCGCCACCATAGAGAGAAGCGAGATG	ACCATGTTGTGACGGTGGCAGAGG
mCol1a1	TGGCAAAGACGGACTCAACGGTCTC	GAAGTCATAACCGCCACTGGGAGGTC
mHas2	ACCCTATGGTTGGAGGTGTTGGAGGA	CACGCTGCTGAGGAAGGAGATCCAG
mActa2	CCTGGAGAAGAGCTACGAACTGCCTGA	TTTCGTGGATGCCCGCTGACTC
mPkp1	TGCTTCAGCAACAGGGGTGACAAGA	CATGAGGTTCAGGTAGGTCCGGATGG
mLif	GCAGCGCCAATGCTCTCTTCATTTC	GCGCACATAGCTTTTCCACGTTGTTG
mP0	TGCACTCTCGCTTTCTGGAGGGTGT	AATGCAGATGGATCAGCCAGGAAGG
hCXCL1	GCCTCAATCCTGCATCCCCCATAGT	GCCTCCTTCAGGAACAGCCACCAGT
hIL6	AGGAACAAGCCAGAGCTGTGCAGATG	TTTGTGGTTGGGTCAGGGGTGGTTA
hCXCL2	CCGCATCGCCCATGGTTAAGAAAAT	GCCTCCTTCAGGAACAGCCACCAAT
hCSF3	GAGCTTCCTGCTCAAGTGCT	CACTCACCAGCTTCTCCTGG
hCOL1A1	TCAGCAAGAACCCCAAGGACAAGAGG	AGGAAGGTCAGCTGGATGGCCACAT
hFN1	CAGTGGAATGCACCACAGCCATCTC	TGGTAGCTTCCTTCCAACGGCCTACA
hP0	CCTTCTCCTTTGGGCTGGTCATCCA	CAGACACTGGCAACATTGCGGACAC

RNA-Seq analysis and bioinformatics

RNA integrity was assessed on an Experion StdSens RNA Chip (Bio-Rad). RNAseq libraries were prepared using the TruSeq Stranded mRNA Library Prep kit (Illumina) and sequenced on an Illumina NextSeq550 platform, High Output Kit v2.5, 50 bases single-reads according to the manufacturer's instructions. The paired-end reads were mapped using salmon v1.3.0[10] against the mouse transcriptome (Ensembl - Mus musculus - release 100) with decoys. The quantifications from salmon were imported into R version 4.0.1 using the tximeta package (version 1.6.2)[11]. The transcript counts were summarized to gene level. The resulting gene level quantifications served as input to DESeq2 v1.28.1[12].

Gene expression levels in qPSC, Tc17-iCAF and DKO-CAF were compared against each other respectively, using default parameters. Gene comparisons with padj < 0.001 were considered differentially expressed. Correction for base gene expression was performed

by subtracting the mean expression values of the qPSC from both Tc17-iCAF and DKO-CAF. All differentially expressed genes (DEG) were stratified into 9 modules dependent on the mutual up- or downregulation in PSC vs Tc17-ICAF vs DKO-CAF. Gene expression profiles were plotted as heatmaps (color-coded z-scores for the regularized logarithm (rlog) transformed, corrected expression values with the R programming language and the pheatmap package (version 1.0.12). Sequencing data has been uploaded to GEO archives under accession number GSE202377.

Gene expression levels in $Panc^{OVA}$ cells after the Tc17-iCAF, TGFβ−myCAF and qPSC co-cultures were compared against each other respectively, using default parameters. Gene comparisons with padj < 0.1 were considered differentially expressed. Correction for base gene expression was performed by subtracting the mean expression values of the qPSC control co-culture from both Tc17-iCAF and TGFβ-myCAF cocultures. All DEG were stratified into 7 defined modules dependent on the mutual up- or downregulation in Tc17-iCAF and TGFβ-myCAF tumor-cell co-culture. Gene expression profiles were plotted as heatmaps (color-coded z-scores for the regularized logarithm (rlog) transformed, corrected expression values with the R programming language and the pheatmap package (version 1.0.12). Sequencing data has been uploaded to GEO archives under accession number GSE182126.

Gene expression levels in $Panc^{OVA}$ cells after the Tc17-iCAF and Tc17 co-cultures were compared against each other respectively, using default parameters. Gene comparisons with padj < 0.001 were considered differentially expressed. Correction for base gene expression was performed by subtracting the mean expression values of the $Panc^{OVA}$ control from both Tc17-iCAF and Tc17 cocultures. All DEG were stratified into 4 defined modules dependent on the mutual up- or downregulation in Tc17-iCAF and Tc17 tumor-cell co-culture. Gene expression profiles were plotted as heatmaps (color-coded z-scores for the regularized logarithm (rlog) transformed, corrected expression values with the R programming language and the pheatmap package (version 1.0.12). Sequencing data has been uploaded to GEO archives under accession number GSE218816.

Molecular Signatures Database Hallmark, Gene Ontology and STRING analysis

Pathway enrichment analysis for Molecular Signatures Database (MSigDB) was performed on all 9 gene modules employing EnrichR[13] referencing MSigDB Hallmark 2020. Top 3 significantly enriched (-log10 padj) MSigDB Hallmark 2020 terms for each module are plotted as bubble graphs in Prism v9. Gene ontology analysis was performed on all gene modules employing EnrichR[13] referencing GO Biological processes. Top significantly enriched (-log10

padj) *biological processes* GO terms for each module are plotted as bubble graphs in Prism v9. To predict an iCAF coculture-driven interactome, the same, significantly upregulated genes of Tc17-iCAF cocultured Panc^{OVA} cells were used as input dataset to STRING v11[14], set to medium confidence, only query proteins, no disconnected nodes, MCL clustering, inflation=3. For further visualization, underlying coloring was added manually.

Gene set enrichment analysis (GSEA)

To validate iCAF specific signatures in Tc17-iCAF vs qPSC vs DKO-CAF cross-mapping to upregulated or downregulated genes (p adj=0.001) in iCAF, which were induced by tumor-derived ligands, comparing to qPSC[15,16] was performed using GSEA (V 4.3.2 Broad Institute, San Diego). To validate tumor specific Tc17-iCAF vs TGFβ-myCAF or Tc17-iCAF vs Tc17 co-culture dependent expression patterns, cross-mapping to LIFR-dependent KPC mouse tumor[17] and human PDAC signatures[18] was performed in GSEA (V 4.3.2 Broad Institute, San Diego). Signatures for murine LIFR-dependent tumor transcripts were extracted from GSE119694[17] and used as reference gene set. The reference expression set for Classical-A or Basal-like A human PDAC tumors was taken from[18]. Enriched genes were plotted as heatmaps (color-coded z-scores for the regularized logarithm (rlog) with the R programming language and the pheatmap package (version 1.0.12).

Tumor models and adoptive T-cell transfer

For the subcutaneous (s.c.) *in vivo* tumor/T cell interaction model (figure 2A-D), 8–12-week-old WT mice were injected with 1×10^6 Panc^{OVA} cells *s.c.* into the left flank. 5 days post-injection, tumor-bearing animals were treated with 1×10^6 Tc17 or CTLs, which had been differentiated for 4 days *in vitro* from naïve CD8$^+$ T cells isolated from OT-1 mice.

For the *s.c. in vivo* tumor cell/primed CAF interaction model (figure 4A-E, I-L)), qPSC, CTL-CAF, Tc17-iCAF and DKO-CAF were generated as described above. Each matrigel droplet, harboring 5×10^5 CAF, was dissolved in 50 µl of ice-cold PBS, mixed with 5×10^5 Panc^{OVA} cells and injected into the flanks of a *Rag1*$^{-/-}$ mouse, or mixed with 5×10^5 PaTu8988T cells and injected s.c. into athymic *Foxn1*$^{nu/nu}$ mice.

For the *s.c. in vivo* CAF priming model (figure 6A-E, supplementary figure 9A-G, supplementary figure 10A-D), a mixture of 5×10^5 WT or *Il17ra*$^{-/-}$qPSC and 5×10^5 Panc$^{OVA.}$ or 5×10^5 KPC tumor cells was applied. Each matrigel droplet harboring 5×10^5 WT or *Il17ra*$^{-/-}$qPSC was dissolved in 50 µl of ice-cold PBS, mixed with 5×10^5 Panc^{OVA} or 5×10^5 KPC-

derived tumor cells and injected into the flanks of either WT or *Il17ra*$^{-/-}$ mice, followed by an *i.p.* injection of *in vitro* differentiated Tc17 cells from either WT or *Il17af*$^{-/-}$ CD8^{+} T cells. Tumor growth was measured daily and was visualized by volume approximation (V=length × width^2/2 in cubic millimeters).

For the orthotopic *in vivo* tumor cell/primed CAF interaction model (figure 4F-H, supplementary figure 6H,I) CD90.1^{+}qPSC and CD90.1^{+}Tc17-iCAF and were generated as described above, and a mixture of 2 × 10^4 CD90.1^{+}qPSC, CD90.1^{+}Tc17-iCAF or CD90.1^{+}DKO-CAF and 2 × 10^4 KPC cells were orthotopically implanted into *Rag1*$^{-/-}$ mice as previously described[19]. Mice were kept anesthetized during all surgical procedures. A 1.5 cm abdominal incision was made, and the pancreas was pulled out from the abdominal cavity. 15µl of DMEM containing 2 × 10^4 KPC tumor cells alone or with 2 × 10^4 CD90.1^{+}qPSC, CD90.1^{+}Tc17-iCAF or CD90.1^{+}DKO-CAF was injected into the pancreas. After injection, the peritoneum was closed using absorbable sutures, and the skin was sealed using a clip. Tumors were monitored weekly using ultrasound (Vevo 2100 Imaging System).

For the orthotopic *in vivo* CAF priming model (figure 6F-H, supplementary figure 9H-J) a mixture of 2 × 10^4 KPC tumor cells ± 2 × 10^4 WT CD90.1^{+}qPSC -were orthotopically implanted into WT C57BL/6J mice. On the next day the mice were *i.p.* injected with *in vitro* differentiated 1 × 10^6 Tc17 cells obtained from either WT or *Il17af*$^{-/-}$ CD8^{+} T cells.

For the orthotopic genetic CAF priming model WT and *Il17a/f*$^{-/-}$ mice (figure 6I-K, supplementary figure 10A) a mixture of 1.5 × 10^4 KPC tumor cells ± 6 × 10^4 CD90.1^{+}qPSC were orthotopically implanted into WT or *Il17a/f*$^{-/-}$C57BL/6J mice.

For the orthotopic *in vivo* CAF priming model (figure 6L-N, supplementary figure 10E,F) a mixture of 2 × 10^4 KPC tumor cells ± 2 × 10^4 WT or *Il17ra*$^{-/-}$ CD90.1^{+}qPSC -were orthotopically implanted into *Il17ra*$^{-/-}$ C57BL/6J mice. On the next day the mice were *i.p.* injected with *in vitro* differentiated 1 × 10^6 Tc17 cells obtained from WT CD8^{+} T cells.

Mice were sacrificed upon poor outcome. Then, tumors were surgically removed and the tumor mass and volume were measured. The tumor volume expressed in cubic millimeters was determined by multiplying the length, the width and the height of surgically removed tumors. After surgical removal, tumors were digested into single-cell solutions by 200 u/ml Collagenase IV (Worthington), 10 µg/ml DNAse 1 (Roche) in HBSS, 37°C, 300 rpm agitation and filtered through 100 µm cell strainers (Sysmex). Subsequently staining using TIL and fibroblasts panels were performed. Based on the expression of fibroblast markers and CD90.1 the CAF populations were sorted on FACSAria III (BD Biosciences) into endogenous or transferred populations and then analyzed for subtype-specific genes by qPCR.

Antibodies for FACS stainings:

Human TIL Panel (supplementary figure 1H,I): Zombie NIR™ Fixable Viability Kit (# 423106 BioLegend), anti-hCD3 AF488 (#317310 BioLegend), anti-hCD4-Pacific Blue (#300521 BioLegend), anti-hCD8 (BV510, BioLegend #344732), hIL-17A (PE #512306 BioLegend) and hIFNγ (APC, #502512 BioLegend).

Murine TIL Panel (figure 2D, supplementary figure 3F,H,I): Zombie NIR™ Fixable Viability Kit (# 423106 BioLegend), anti-mCD8α (AF488 #557668 BD Bioscience), anti-mCD4 (Pacific Blue #558107 BD Bioscience), anti-mCD45.2 APC (#109814 BioLegend), anti-mIL-17A (PE #12-7177-81 or APC #17-7177-81 eBioscience), and IFNγ (PerCp-Cy5.5 #505822 or APC #502810 BioLegend)

Fibroblast/Sort Panel (Figure 4D,E,H,K,L 6D,E,H,K,N, supplementary figure 6C,D,E,H 9D,E,F, 10D,E): 7-Aminoactinomycin D (7-AAD) PerCP (#A1310 Thermo Fisher), anti-mEPCAM AF488 (#118210 BioLegend), anti-mCD45 PE (#103106 Biolegend), anti-mPDPN APC (#127410 BioLegend), anti-mCD90.1 BV500 (#202535 Biolegend), anti-mLy6c BV421 (48593182 eBioscience).

Fibroblast IL-17 Receptor Panel (Figure 3D, supplementary figure 3E,G,7G): Zombie NIR™ Fixable Viability Kit (# 423106 BioLegend), anti-mIL-17RA PE (eBioscience #12-7182-82), anti-mIL-17RC APC (#FAB2270A R&D Systems), Rat IgG2a, κ Isotype Control PE (#554689 BD Biosciences), Goat IgG Isotype Control APC (#403006 BioLegend), for human PSC (Figure 4A); anti-hIL-17RA PE (#FAB177P R&D Systems), anti-hIL-17RC APC (#FAB22691A R&D Systems), MouseIgG1 κ Iso Control PE (#12-4714-42 eBiosciences) and Mouse IgG2b κ Iso Control APC (#555745 BD Pharmingen) for human PSC.

Statistics

For statistical analysis, GraphPad Prism v10 was used. Data are presented as bar graphs (mean ± s.d) or as tumor growth curves (mean ± s.e.m.). Each data point represents one biological replicate except for Figure 2F in which 6 technical replicates representative for 3 independent experiments are shown. Normality of distribution and homogeneity of variances was evaluated by Shapiro-Wilk test and Brown-Forsythe, respectively for all datasets. Statistical significance to compare two groups was evaluated using two-tailed/unpaired *t*-tests. In case of datasets not conforming to normality criteria, nonparametric Mann-Whitney tests were used. The chosen confidence interval for all test was 95%. For multiple groups and/or multiple condition comparisons, one-way or two-way analysis of variance (ANOVA) was performed followed by a Tukey`s HSD, Dunnett's or Bonferroni post hoc test, respectively. Datasets lacking

continuous values were analyzed by mixed-effects model (REML) with Tukey`s HSD post-test. For datasets not conforming to normality criteria, nonparametric Kruskal-Wallis test was used. A critical value for significance of $P < 0.05$ (*) was used throughout the study, and statistical thresholds of $P < 0.01$ (**), $P < 0.001$ (***), as well as $P < 0.0001$ (****) are indicated in the figures by asterisks.

Patient data analysis

Statistical data analysis was performed using MedCalc Version 20.006 (MedCalc Software, Ostend, Belgium). Mann-Whitney U test was used for comparison of independent continuous variables (Figures 1C, S1C-E, S2C,D,F, S3C,D, table 1 and 4, Age and Tumor size). Chi-square test was used for comparison of frequencies between groups (table 1 and 4 Gender, T, N, G and UICC stage). Correlation analyses were performed using Spearman's rank correlation test. Survival curves were estimated using the Kaplan–Meier method and compared by log-rank test (n=71 PDAC patients with known survival time). A Cox proportional hazard model was employed to identify the independent predictors of survival. The variables $CD8^+IL\text{-}17A^+$ cell infiltration (≤ 5 versus > 5 $CD8^+IL\text{-}17A^+$ cells/mm^2) or $CD8^+ROR\gamma t^+$ cell infiltration (≤ 6 versus > 6 $CD8^+ROR\gamma t^+$ cells/mm^2) or $CD4^+ROR\gamma t^+$ cell infiltration (≤ 9 versus > 9 $CD4^+ROR\gamma t^+$ cells/mm^2), T (extent of primary tumor, T1-2 versus T3-4), N (regional lymph node metastases, N0 versus N+), and G (grading, G1-2 vs. G3-4) were entered in the Cox model in one single step (enter method, n=68 PDAC patients with known Tc17, T, N, G strata), (enter method, n=71 PDAC patients with known Th17, T, N, G strata). Values of $P < 0.05$ were considered statistically significant. For analyses of $CD8^+ROR\gamma t^+$, $CD8^+IL\text{-}17A^+$, $CD8^+$, $IL\text{-}17A^+$, $CD4^+ROR\gamma t^+$, cells as well as for ratios $CD8^+ROR\gamma t^+/CD8^+$ and $CD8^+IL\text{-}17A^+/CD8^+$ median values were used as cut-off. For tumor size the value of 4 cm was chosen as a cut-off, because this is the difference in tumor diameter between T2 vs T3 tumors according to the 8th TNM AJCC/UICC classification. For GATA6 cut-off 80 was chosen because of a very high median value (93.3333) and for CK5 cut-off 5 was chosen because of a very low median value (1.2500).

Study approval

The murine study was approved by the regional agency on animal experimentation (Regierungspräsidium Giessen). For human samples, approval was given by local Ethics Committee responsible (Landesärztekammer RLP for TMAs, Landesärztekammer Hessen for fresh PDAC samples).

References:

1. O'Kane GM, Grunwald BT, Jang GH*, et al.* GATA6 Expression Distinguishes Classical and Basal-like Subtypes in Advanced Pancreatic Cancer. *Clin Cancer Res* **26**, 4901-4910 (2020).

2. El Malki K, Karbach SH, Huppert J*, et al.* An alternative pathway of imiquimod-induced psoriasis-like skin inflammation in the absence of interleukin-17 receptor a signaling. *J Invest Dermatol* **133**, 441-451 (2013).

3. Luu M, Riester Z, Baldrich A*, et al.* Microbial short-chain fatty acids modulate CD8(+) T cell responses and improve adoptive immunotherapy for cancer. *Nat Commun* **12**, 4077 (2021).

4. Elsasser HP, Lehr U, Agricola B*, et al.* Establishment and characterisation of two cell lines with different grade of differentiation derived from one primary human pancreatic adenocarcinoma. *Virchows Arch B Cell Pathol Incl Mol Pathol* **61**, 295-306 (1992).

5. Hingorani SR, Wang L, Multani AS*, et al.* Trp53R172H and KrasG12D cooperate to promote chromosomal instability and widely metastatic pancreatic ductal adenocarcinoma in mice. *Cancer Cell* **7**, 469-483 (2005).

6. Boj SF, Hwang CI, Baker LA*, et al.* Organoid models of human and mouse ductal pancreatic cancer. *Cell* **160**, 324-338 (2015).

7. Neesse A, Wagner M, Ellenrieder V*, et al.* Pancreatic stellate cells potentiate proinvasive effects of SERPINE2 expression in pancreatic cancer xenograft tumors. *Pancreatology* **7**, 380-385 (2007).

8. Jesnowski R, Furst D, Ringel J*, et al.* Immortalization of pancreatic stellate cells as an in vitro model of pancreatic fibrosis: deactivation is induced by matrigel and N-acetylcysteine. *Lab Invest* **85**, 1276-1291 (2005).

9. Campos Carrascosa L, Klein M, Kitagawa Y*, et al.* Reciprocal regulation of the Il9 locus by counteracting activities of transcription factors IRF1 and IRF4. *Nat Commun* **8**, 15366 (2017).

10. Patro R, Duggal G, Love MI*, et al.* Salmon provides fast and bias-aware quantification of transcript expression. *Nat Methods* **14**, 417-419 (2017).

11. Love MI, Soneson C, Hickey PF*, et al.* Tximeta: Reference sequence checksums for provenance identification in RNA-seq. *PLoS Comput Biol* **16**, e1007664 (2020).

12. Love MI, Huber W, Anders S. Moderated estimation of fold change and dispersion for RNA-seq data with DESeq2. *Genome Biol* **15**, 550 (2014).

13. Xie Z, Bailey A, Kuleshov MV*, et al.* Gene Set Knowledge Discovery with Enrichr. *Curr Protoc* **1**, e90 (2021).

14. Szklarczyk D, Gable AL, Lyon D*, et al.* STRING v11: protein-protein association networks with increased coverage, supporting functional discovery in genome-wide experimental datasets. *Nucleic Acids Res* **47**, D607-D613 (2019).

15. Biffi G, Oni TE, Spielman B*, et al.* IL1-Induced JAK/STAT Signaling Is Antagonized by TGFbeta to Shape CAF Heterogeneity in Pancreatic Ductal Adenocarcinoma. *Cancer Discov* **9**, 282-301 (2019).

16. Ohlund D, Handly-Santana A, Biffi G*, et al.* Distinct populations of inflammatory fibroblasts and myofibroblasts in pancreatic cancer. *J Exp Med* **214**, 579-596 (2017).

17. Shi Y, Gao W, Lytle NK*, et al.* Targeting LIF-mediated paracrine interaction for pancreatic cancer therapy and monitoring. *Nature* **569**, 131-135 (2019).

18. Chan-Seng-Yue M, Kim JC, Wilson GW*, et al.* Transcription phenotypes of pancreatic cancer are driven by genomic events during tumor evolution. *Nat Genet* **52**, 231-240 (2020).

19. Tu M, Klein L, Espinet E*, et al.* TNF-alpha-producing macrophages determine subtype identity and prognosis via AP1 enhancer reprogramming in pancreatic cancer. *Nat Cancer* **2**, 1185-1203 (2021).

20. Mucciolo G, Curcio C, Roux C*, et al.* IL17A critically shapes the transcriptional program of fibroblasts in pancreatic cancer and switches on their protumorigenic functions. *Proc Natl Acad Sci U S A* **118**, (2021).

2. Supplementary Tables 1-6.

Table 1. Characteristics of PDAC patients: CD8⁺IL-17A⁺ and CD8⁺RORγt⁺ cells

Parameter	Total (N=112)	CD8⁺IL-17A⁺ ≤ 5 /mm² (N= 53)	CD8⁺IL-17A⁺ > 5 /mm² (N= 59)	*P*-value	CD8⁺RORγt⁺ ≤ 6/mm² (N=60)	CD8⁺RORγt⁺ > 6 /mm² (N=51)	*P*-value
Gender							
male	56 (50.0%)	27 (50.9%)	29 (49.2%)	0.8506	27 (45.0%)	29 (56.9%)	0.2149
female	56 (50.0%)	26 (49.1%)	30 (50.8%)		33 (55.0%)	22 (43.1%)	
Age [years]*	69 (62 – 74)	69 (62 – 73)	69 (62 – 75)	0.6262	67.5 (61.5 – 73)	70 (62.25 – 75)	0.4188
T category							
pT 1	10 (8.9%)	6 (11.3%)	4 (6.8%)	0.0314	7 (11.7%)	3 (5.9%)	0.0930
pT 2	66 (58.9%)	35 (66.0%)	31 (52.5%)		37 (61.7%)	28 (54.9%)	
pT 3	29 (25.9%)	7 (13.2%)	22 (37.3%)		10 (16.7%)	19 (37.3%)	
pT 4	1 (0.9%)	1 (1.9%)	0 (0.0%)		1 (1.7%)	0 (0.0%)	
n.a.	6 (5.4%)	4 (7.5%)	2 (3.4%)		5 (8.3%)	1 (2.0%)	
N category							
pN 0	37 (33.0%)	22 (41.5%)	15 (25.4%)	0.0313	24 (40.0%)	12 (23.5%)	0.0258
pN 1	41 (36.6%)	20 (37.7%)	21 (35.6%)		23 (38.3%)	18 (35.3%)	
pN 2	32 (28.6%)	9 (17.0%)	23 (39.0%)		11 (18.3%)	21 (41.2%)	
n.a.	2 (1.8%)	2 (3.8%)	0 (0.0%)		2 (3.3%)	0 (0.0%)	
Grading							
G1	5 (4.5%)	4 (7.5%)	1 (1.7%)	0.1768	4 (6.7%)	1 (2.0%)	0.4125
G2	62 (55.4%)	32 (60.4%)	30 (50.8%)		33 (55.0%)	28 (54.9%)	
G3	42 (37.5%)	16 (30.2%)	26 (44.1%)		20 (33.3%)	22 (43.1%)	
G4	1 (0.9%)	0 (0.0%)	1 (1.7%)		1 (16.7%)	0 (0.0%)	
n.a.	2 (1.8%)	1 (1.9%)	1 (1.7%)		2 (3.3%)	0 (0.0%)	
UICC stage							
UICC I	29 (25.9%)	19 (35.8%)	10 (16.9%)	0.0524	20 (33.3%)	8 (15.7%)	0.0610
UICC II	43 (38.4%)	20 (37.7%)	23 (39.0%)		23 (38.3%)	20 (39.2%)	
UICC III	30 (26.8%)	10 (18.9%)	20 (33.9%)		11 (18.3%)	19 (37.3%)	
UICC IV	5 (4.5%)	1 (1.9%)	4 (6.8%)		2 (3.3%)	3 (5.9%)	
n.a.	5 (4.5%)	3 (5.7%)	2 (3.4%)		4 (6.7%)	1 (2.0%)	
Tumor size [cm]*	3.4 (2.5 – 4.5) (n.a. in 6 patients)	3.0 (2.5 – 3.8) (n.a. in 4 patients)	3.8 (2.8 – 5.0) (n.a. in 2 patients)	0.0065	3.0 (2.5 – 3.8) (n.a. in 5 patients)	4.0 (2.8 – 5.0) (n.a. in 1 patient)	0.0083

*Presented as median with (interquartile range). *P* values are from Chi-square test (Gender, T, N, G, UICC stage or Mann-Whitney test (Age, Tumor size).

Table 2. Multivariate Cox-regression analysis of PDAC patients of overall survival for CD8⁺IL-17A⁺ cells (Overall Model Fit significance level *P*=0.0015, n=69)

Multivariate Cox regression analysis			
Factor	Strata	*P*-value	HR (95%CI)
$CD8^+IL\text{-}17A^+$	> 5/mm² vs. ≤ 5/mm²	0.0033	2.44 (1.35-4.41)
T	≥3 vs. ≤2	0.4060	1.29 (0.71-2.33)
N	+ vs. 0	0.7814	1.08 (0.62-1.89)
Grading	≥3 vs. ≤2	0.2189	1.45 (0.80-2.62)

Table 3. Multivariate Cox-regression analysis of PDAC patients of overall survival for $CD8^+ROR\gamma t^+$ cells (Overall Model Fit significance level *P*= 0.0032, n=68)

Multivariate Cox regression analysis			
Factor	Strata	*P*-value	HR (95%CI)
$CD8^+ROR\gamma t^+$	> 6/mm² vs. ≤ 6/mm²	0.0053	2.22 (1.26-3.89)
T	≥3 vs. ≤2	0.4255	1.27 (0.71-2.28)
N	+ vs. 0	0.6709	1.13 (0.64-1.98)
Grading	≥3 vs. ≤2	0.2104	1.45 (0.81-2.58)

Table 4. Characteristics of PDAC patients: $CD4^+ROR\gamma t^+$ cells

Parameter	**Total (N=111)**	**$CD4^+ROR\gamma t^+$ ≤ 9/mm² (N=47)**	**$CD4^+ROR\gamma t^+$ > 9/mm² (N=64)**	***P*-value**
Gender				
male	56 (50.0%)	26 (45.0%)	30 (56.9%)	0.3815
female	56 (50.0%)	21 (55.0%)	34 (43.1%)	
Age [years]*	69 (62 – 74)	70 (61.25 – 73)	67.5 (62 – 75)	0.7335
T category				
pT 1	10 (8.9%)	2 (4.3%)	8 (12.5%)	0.2585
pT 2	66 (58.9%)	30 (63.8%)	35 (54.7%)	
pT 3	29 (25.9%)	11 (23.4%)	18 (28.1%)	
pT 4	1 (0.9%)	1 (2.1%)	0 (0.0%)	
n.a.	6 (5.4%)	3 (6.4%)	3 (4.7%)	
N category				
pN 0	37 (33.0%)	19 (40.0%)	17 (26.6%)	0.0060
pN 1	41 (36.6%)	21 (38.3%)	20 (31.3%)	
pN 2	32 (28.6%)	6 (18.3%)	26 (40.6%)	
n.a.	2 (1.8%)	1 (3.3%)	1 (1.6%)	
Grading				
G1	5 (4.5%)	1 (6.7%)	4 (6.3%)	0.4328
G2	62 (55.4%)	29 (55.0%)	32 (50.0%)	
G3	42 (37.5%)	16 (33.3%)	26 (40.6%)	
G4	1 (0.9%)	0 (16.7%)	1 (1.6%)	
n.a.	2 (1.8%)	1 (3.3%)	1 (1.6%)	
UICC stage				
UICC I	29 (25.9%)	15 (33.3%)	13 (20.3%)	0.0120
UICC II	43 (38.4%)	22 (38.3%)	21 (32.8%)	
UICC III	30 (26.8%)	7 (18.3%)	23 (35.9%)	
UICC IV	5 (4.5%)	0 (3.3%)	5 (7.8%)	
n.a.	5 (4.5%)	3 (6.7%)	2 (3.1%)	
Tumor size [cm]*	3.4 (2.5 – 4.5) (n.a. in 6 patients)	3.2 (2.5 – 4.2) (n.a. in 3 patients)	3.5 (2.5 – 4.5) (n.a. in 3 patients)	0.4721

*Presented as median with (interquartile range). P values are from Chi-square test (Gender, T, N, G, UICC stage or Mann-Whitney test (Age, Tumor size).

Table 5. Multivariate Cox-regression analysis of PDAC patients of overall survival for CD4$^+$RORγt$^+$ cells (Overall Model Fit significance level *P*=0.0176, n=68)

Multivariate Cox regression analysis			
Factor	Strata	*P*-value	HR (95%CI)
CD4$^+$RORγt$^+$	> 9/mm^2 vs. ≤ 9/mm^2	0.0512	1.74 (1.00-3.04)
T	≥3 vs. ≤2	0.1067	1.62 (0.90-2.90)
N	+ vs. 0	0.5789	1.17 (0.67-2.04)
Grading	≥3 vs. ≤2	0.1161	1.60 (0.89-2.86)

Table 6. Multivariate Cox-regression analysis of PDAC patients of overall survival for CD4$^+$ RORγt$^+$and CD8$^+$RORγt$^+$ cells (Overall Model Fit significance level *P*=0.0050, n=68)

Multivariate Cox regression analysis			
Factor	Strata	*P*-value	HR (95%CI)
CD4$^+$RORγt$^+$	> 9/mm^2 vs. ≤ 9/mm^2	0.3387	1.35 (0.73-2.47)
CD8$^+$RORγt$^+$	> 6/mm^2 vs. ≤ 6/mm^2	0.0307	1.96 (1.06-3.61)
T	≥3 vs. ≤2	0.3261	1.35 (0.74-2.46)
N	+ vs. 0	0.6555	1.14 (0.65-1.99)
Grading	≥3 vs. ≤2	0.1991	1.47 (0.82-2.63)

3. Supplementary Figures 1-10

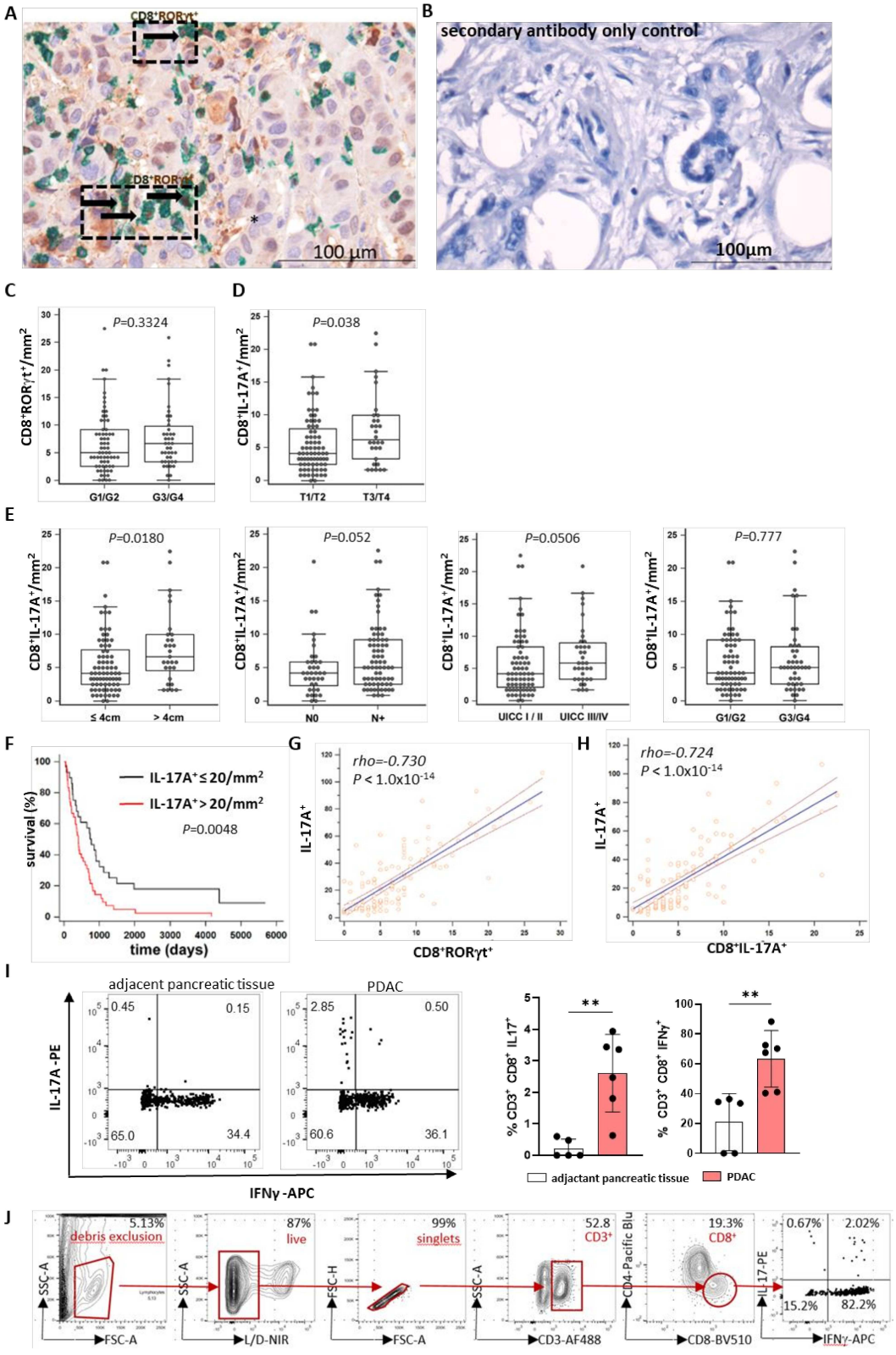

Supplementary Figure 1. Tc17 cells associate with tumor size, metastases and staging in PDAC. (A) Double immunostaining of PDAC tissue sections with beginning anaplasia was performed using antibodies against CD8α (green) and RORγt (brown), scale bar 100 µm. (B) Control staining with secondary antibody only of PDAC tissue, scale bar 100 µm. (C) $CD8^+$ $ROR\gamma t^+$ cell frequency per mm^2 in tumors with grading G1/G2 vs G3/G4 (n=109). (D) $CD8^+$ $IL\text{-}17A^+$ cell frequency per mm^2 in T1/2 vs T3/T4 tumors (n=106). (E) $CD8^+$ $IL\text{-}17A^+$ cell frequency per mm^2 in tumors ≤ 4 cm vs > 4 cm (n=106), N0 vs N+ tumors (n=110), UICC stage I/II vs III/IV (n=107) and tumor grading G1/G2 vs G3/G4 (n=110). (C-E) Box-plots depict the lower and upper adjacent values (whiskers) and the upper and lower quartiles (top and bottom edges of the box). The median is identified by a horizontal line inside the box, *P* value by Mann-Whitney U test. Each dot represents one individual. (F) Kaplan-Meier curve of overall survival (survival %) of patients with surgically resected PDAC showing ≤ 20/mm^2 vs > 20/mm^2 $IL\text{-}17A^+$ cell infiltration (n=71, *P* values determined by log-rank test). (G,H) Linear regression analysis for frequencies $CD8^+ROR\gamma t^+$ vs $IL\text{-}17A^+$ cells (G) and $CD8^+IL\text{-}17A^+$ vs $IL\text{-}17A^+$ (H) in PDAC tissue. Linear regression line, Spearman's correlation coefficient (rho), and respective P values are shown on the plot (n=111). (I) FACS analysis of $IL\text{-}17^+$ and $IFN\gamma^+$ $CD8^+$ T cells, after restimulation with PMA/Ionomycin for 5h, brefeldin A was added for the last 3h, in adjacent or malignant pancreatic tissue, gated $CD3^+$ $CD8^+$ T cells are shown (mean ± s.d n=5-6). Left, representative FACS plots, right, quantification of $IL\text{-}17A^+$ or $IFN\gamma^+$ $CD3^+CD8^+$ T cell frequency is shown. (J) Gating strategy for FACS analysis of human fresh PDAC tissue samples. Acquired cells were first gated for exclusion of debris (SSC-A vs FSC-A), following by gating for living cells (L/D vs SSC-A) and then for single cells (FSC-H vs FSC-A). $CD8^+$ T cells were identified based on the expression of CD3, then on CD8 marker (CD4 vs CD8). % of calculated $CD8^+$ cells is based on the $CD3^+$ gate. $CD8^+$ T cells were then analyzed for the intracellular production of IFNγ- and IL-17A after restimulation with PMA and ionomycin in the presence of brefeldin A. In (I) each dot represents one individual, statistic evaluated by Mann-Whitney-U test, **P<0.01.

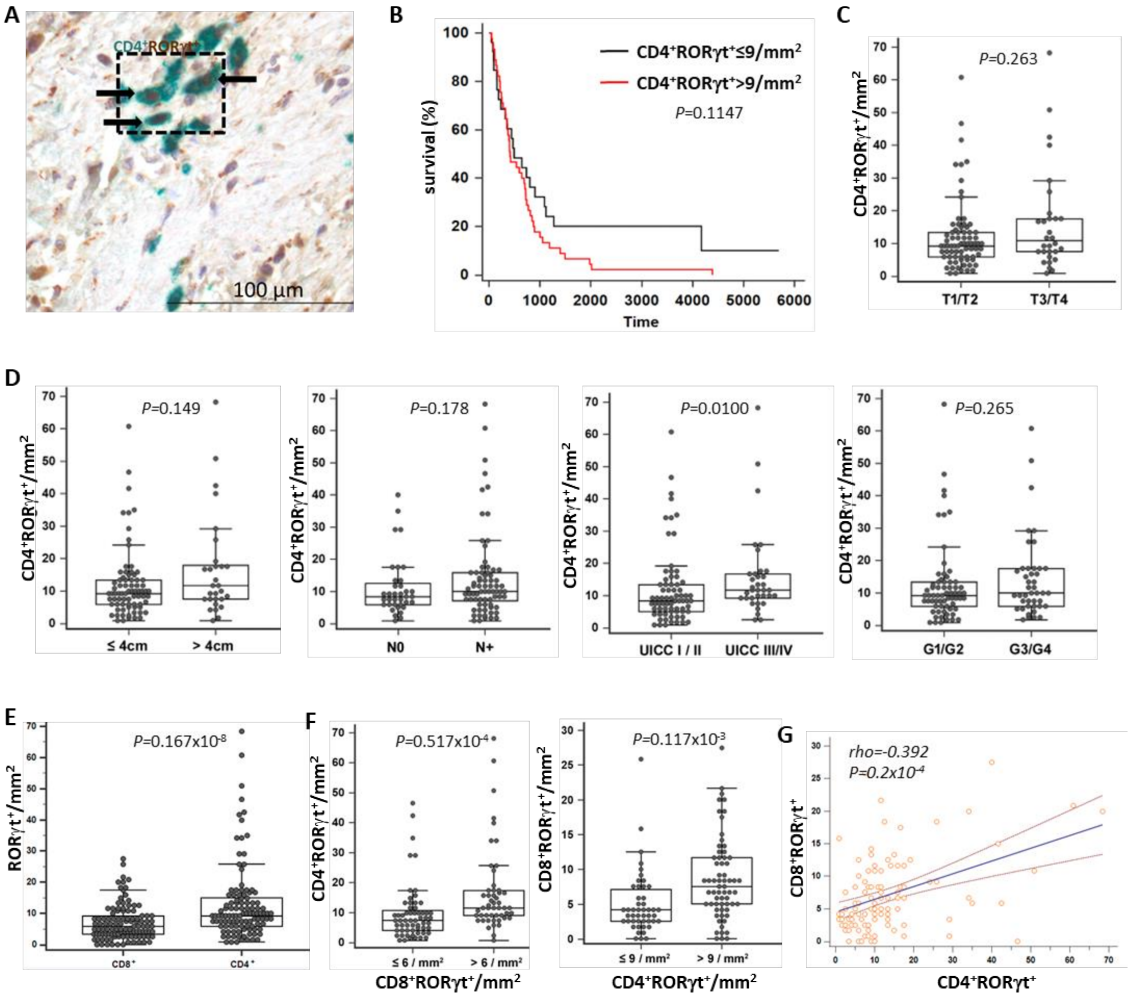

Supplementary Figure 2. Th17 prevalence associates with advanced tumor stage but not with shorter survival in PDAC. (A) Double immune staining of PDAC tissue was performed for CD4 (green) and RORγt (brown), scale bar 100 µm. (B) Kaplan-Meier curve of overall survival (survival %) of patients with surgically resected PDAC showing ≤ 9/mm^2 vs > 9/mm^2 CD4$^+$RORγt$^+$ cell infiltration (n=71, *P* values determined by log-rank test). (C) CD4$^+$RORγt$^+$ cell number per mm^2 in T1/2 vs T3/T4 tumors (n=105). (D) CD4$^+$RORγt$^+$ cell frequency per mm^2 in tumors ≤ 4 cm vs > 4 cm (n=105), N0 vs N+ tumors (n=109) and UICC stage I/II vs III/IV (n=106) and in tumors with grading G1/G2 vs G3/G4 (n=109). (C, D) Box-plots depict the lower and upper adjacent values (whiskers) and the upper and lower quartiles (top and bottom edges of the box). The median is identified by a horizontal line inside the box, *P* value by Mann-Whitney U test. Each dot represents one individual. (E) Numbers of CD4$^+$ vs CD8$^+$ RORγt$^+$ cells per mm^2 tumor tissue from patients with surgically resected PDAC (n=111). (F) Numbers of CD4$^+$RORγt$^+$ cells per mm^2 in tumors with ≤ 6 vs > 6 CD8$^+$RORγt$^+$ cells/mm^2 or

of $CD8^+ROR\gamma t^+$ cells per mm^2 in tumors with ≤ 9 vs > 9 $CD4^+ROR\gamma t^+$ cells/mm^2 from patients with surgically resected PDAC (n=111). (E, F) Box-plots depict the lower and upper adjacent values (whiskers) and the upper and lower quartiles (top and bottom edges of the box). The median is identified by a horizontal line inside the box. (E) *P* value by Wilcoxon test (paired samples). (F) *P* value by Mann-Whitney U test. Each dot represents one individual. (G) Linear regression analysis of $CD8^+ROR\gamma t^+$ vs $CD4^+ROR\gamma t^+$ cell frequencies in PDAC tissue. Linear regression line, Spearman´s correlation coefficient rho, and respective P values are shown on the plot (n=111).

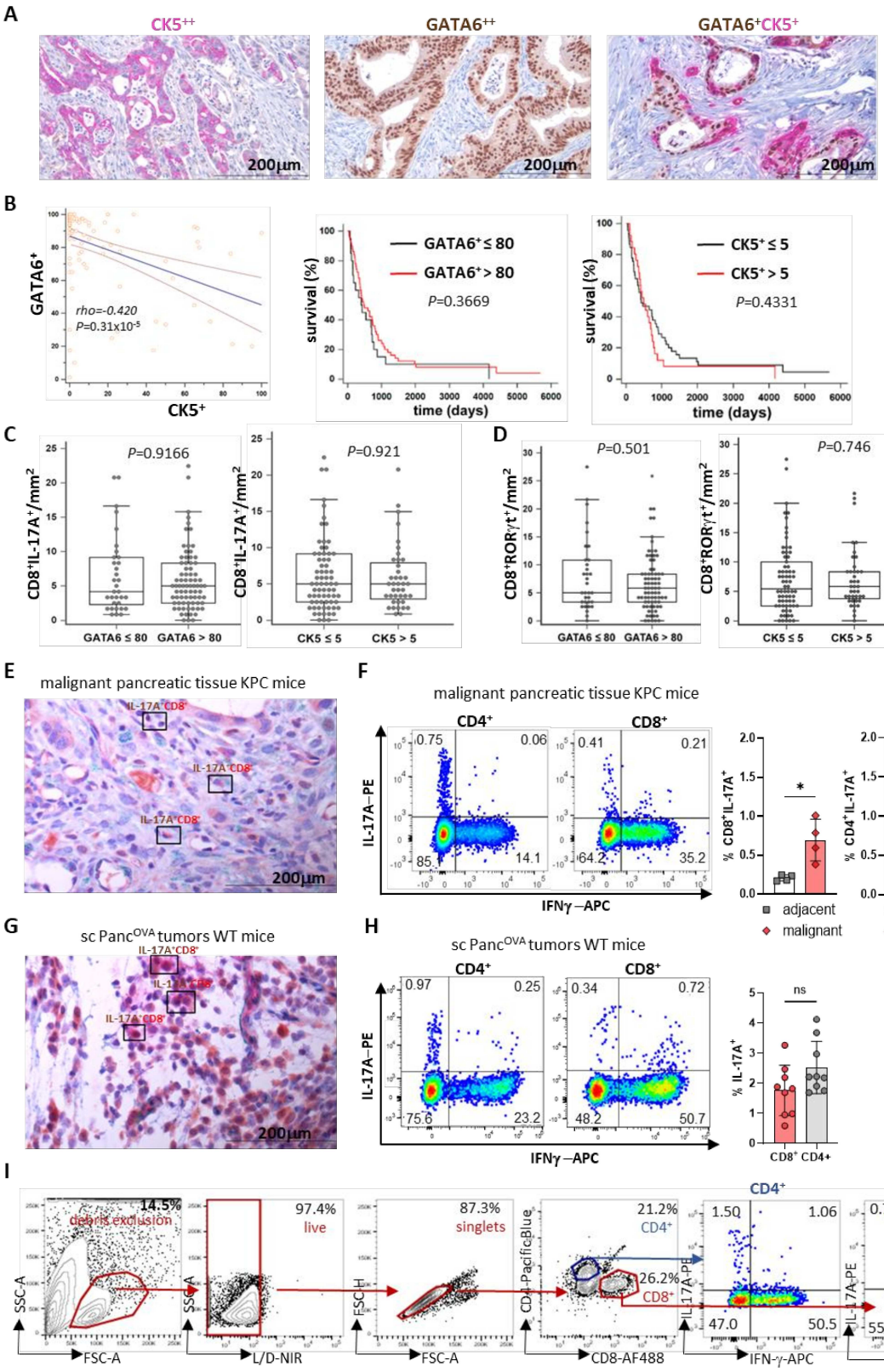
A
CK5++
GATA6++
GATA6+CK5+
200µm
B
GATA6+
rho=-0.420
P=0.31x10-5
CK5+
GATA6+≤ 80
GATA6+> 80
P=0.3669
survival (%)
time (days)
CK5+≤ 5
CK5+> 5
P=0.4331
C
CD8+IL-17A+/mm2
P=0.9166
GATA6 ≤ 80
GATA6 > 80
P=0.921
CK5 ≤ 5
CK5 > 5
D
CD8+RORγt+/mm2
P=0.501
P=0.746
E
malignant pancreatic tissue KPC mice
IL-17A+CD8+
F
CD4+
CD8+
IL-17A–PE
IFNγ –APC
0.75
0.06
85.1
14.1
0.41
0.21
64.2
35.2
% CD8+IL-17A+
% CD4+IL-17A+
*
ns
adjacent
malignant
G
sc PancOVA tumors WT mice
H
0.97
0.25
75.6
23.2
0.34
0.72
48.2
50.7
% IL-17A+
CD8+ CD4+
I
14.5%
debris exclusion
97.4%
live
87.3%
singlets
21.2%
CD4+
26.2%
CD8+
1.50
1.06
47.0
50.5
0.72
0.94
55.1
43.3
SSC-A
FSC-A
L/D-NIR
FSC-H
CD4-PacificBlue
CD8-AF488
IL-17A-PE
IFN-γ-APC

Supplementary Figure 3. Tc17 are present in murine cancer models. (A) Double-staining of PDAC tissue was performed for CK5 (red) and GATA6 (brown); scale bar 200 µm. (B) Left, linear regression analysis of $CK5^+$ vs $GATA6^+$ tumor cell frequencies expressed as percentage of total tumor cells in PDAC tissue as described previously[1]. Linear regression line, Spearman´s correlation coefficient (rho) and respective P values are shown on the plot (n=110). Right, Kaplan-Meier curve of overall survival (survival %) of patients with surgically resected PDAC showing ≤ 80 vs > 80 $GATA6^+$ or of ≤ 5 vs > 5 $CK5^+$ tumor cell frequency expressed as percentage of total tumor cells in PDAC tissue as described previously[1] (n=71, *P* values determined by log-rank test). (C) $CD8^+$ $IL\text{-}17A^+$ cell frequency per mm^2 in $GATA6^+$ ≤ 80 vs ≥ 80 (n=110) or in $CK5^+$ ≤ 5 vs ≥ 5 tumors (n=110). (D) $CD8^+ROR\gamma^+$ cell frequency per mm^2 in $CK5^+$ ≤ 5 vs ≥ 5 (n=110) or in $GATA6^+$ ≤ 80 vs ≥ 80 tumors (n=110). (C, D) Box-plots depict the lower and upper adjacent values (whiskers) and the upper and lower quartiles (top and bottom edges of the box). The median is identified by a horizontal line inside the box, *P* value by Mann-Whitney U test. Each dot represents one individual. (E, G) Double immune staining for $CD8^+$ (red) and $IL\text{-}17A^+$ (brown) cells in pancreatic tumors from KPC mice (E) or in subcutaneous $Panc^{OVA}$ tumors (G), scale bar 200 µm. (F,H) FACS analysis of $IL\text{-}17A^+$ and $IFN\gamma^+$ $CD4^+$ and $CD8^+$ T cells in adjacent healthy or malignant pancreatic tissue from KPC mice (mean ± s.d, n=4) (F) and in subcutaneous $Panc^{OVA}$ tumors from WT mice (mean ± s.d, n=9) (H). Gated $CD8^+$ or $CD4^+$ T cells after restimulation with PMA/Ionomycin in the presence of brefeldin A for 4 h are shown. Left, representative FACS plots, right, quantification of $IL\text{-}17A^+$ $CD4^+$ or $IL\text{-}17A^+$ $CD8^+$ T cell frequency is shown. (I) Gating strategy for FACS analysis of murine tumor tissue samples. Acquired cells were first gated for exclusion of debris (SSC-A vs FSC-A), followed by gating for living cells (L/D vs SSC-A) and then for single cells (FSC-H vs FSC-A). $CD8^+$ T cells were identified based on the expression of CD8 marker (CD4 vs CD8). % of calculated $CD4^+$ and $CD8^+$ cells is based on the single-cell gate.$CD8^+$ T cells were then analyzed for the intracellular production of IFNγ and IL-17A after restimulation with PMA/ionomycin in the presence of brefeldin A. In (F,H) biological replicates are plotted. In (F,H) statistic was evaluated by two-tailed, unpaired *t*-test *P<0.05, ns (not significant).

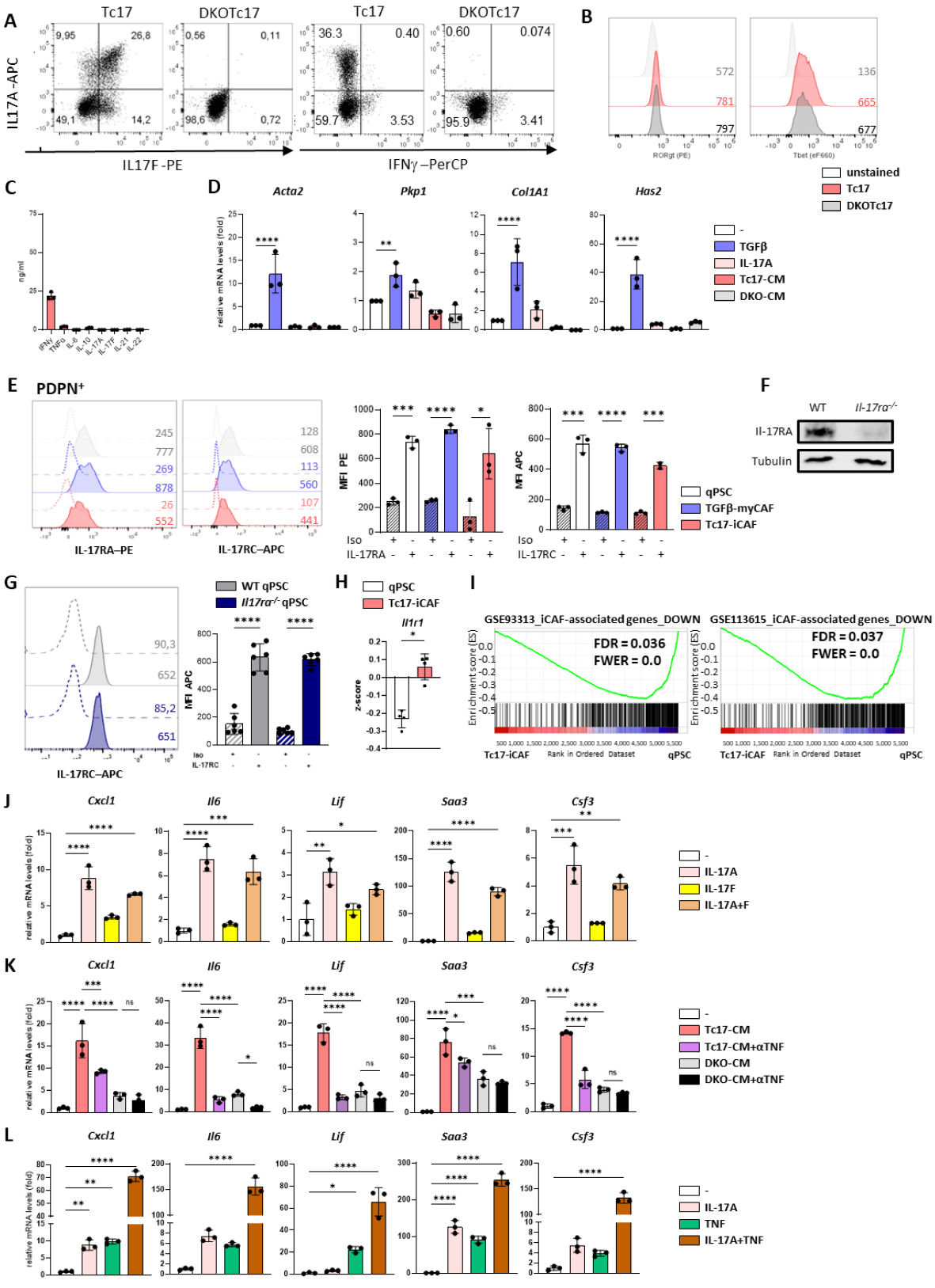
A
Tc17
DKOTc17
IL17A -APC
IL17F -PE
IFNγ –PerCP
B
unstained
Tc17
DKOTc17
C
D
Acta2
Pkp1
Col1A1
Has2
TGFβ
IL-17A
Tc17-CM
DKO-CM
E
PDPN+
IL-17RA–PE
IL-17RC–APC
qPSC
TGFβ-myCAF
Tc17-iCAF
F
WT
Il-17ra-/-
Il-17RA
Tubulin
G
WT qPSC
Il17ra-/- qPSC
H
qPSC
Tc17-iCAF
Il1r1
I
GSE93313_iCAF-associated genes_DOWN
FDR = 0.036
FWER = 0.0
GSE113615_iCAF-associated genes_DOWN
FDR = 0.037
FWER = 0.0
J
Cxcl1
Il6
Lif
Saa3
Csf3
IL-17A
IL-17F
IL-17A+F
K
Tc17-CM
Tc17-CM+αTNF
DKO-CM
DKO-CM+αTNF
L
TNF
IL-17A+TNF

Supplementary Figure 4. Tc17 cells via synergism of IL-17A and TNF promote murine iCAF differentiation. (A, B) Purified $CD8^+$ T cells isolated from WT or IL-17A/F DKO mice were activated with anti-CD3/CD28 antibodies in the presence of TGFβ+IL-6 for four days. Tc17 differentiation was confirmed by intracellular staining for IL-17A, IL-17F and IFNγ. Representative FACS plots are shown (A) and by intranuclear staining for RORγt and Tbet. Representative histograms are shown (B). The numbers within the histograms indicate mean fluorescence intensity (MFI). (C) Quantification of cytokines (ng/ml) produced by *in vitro* differentiated IL-17A/F DKO Tc17 cells after restimulation with anti-CD3 antibodies for 24h (n=3). (D) qPCR for indicated transcripts were performed from qPSC incubated with control medium (-), control medium +2 ng/ml TGFβ (TGFβ), 50 ng/ml anti-IL-17A (IL-17A), 30% of Tc17-CM (Tc17-CM) or 30% CM obtained from IL-17A/F DKO Tc17 cells (DKO-CM) for 48h (mean ± s.d., n=3). Fold of mRNA expression is shown, normalised to the control (-), which was arbitrarily set to 1. (E) FACS analysis showing IL-17RA and IL-17RC levels (MFI) of $PDPN^+$ qPSC, TGFβ-myCAF and Tc17-iCAF (mean ± s.d., n=3). Left, representative histograms, right, quantification of IL-17RA and IL-17RC levels is shown. (F) Western blot analysis of IL-17RA in IL-17RA knockout PSC and WT controls. Loading control, Tubulin (one representative of three independent experiments). (G) FACS analysis for IL-17RC levels (MFI) by WT and *Il17ra*$^{-/-}$ qPSC (mean ± s.d., n=6). Left, representative histograms, right, quantification of IL-17RC levels is shown. (H) z-score for *Il1r1* of qPSC and Tc17-iCAF from RNA-Seq data from figure 3F (mean ± s.d., n=4). (I) Gen set enrichment analysis (GSEA) for differential expression of genes downregulated in iCAF- on raw data RNA-Seq GSE93313 or GSE113615 in Tc17-iCAF vs qPSC. (J) qPCR analysis for indicated gene expression by qPSC incubated with control medium (-), 50 ng/ml IL-17A (IL-17A), 50 ng/ml IL-17F (IL-17F) or 50 ng/ml IL-17A + 50 ng/ml IL-17F (IL-17A+F) for 48h (mean ± s.d., n=3). Fold of mRNA expression is shown, normalised to the control (-), which was arbitrarily set to 1. (K) qPCR analysis for indicated gene expression by qPSC incubated with control medium (-), 30% of Tc17-CM (Tc17CM) 30% Tc17-CM+ 5µg/ml anti-TNF antibodies (Tc17-CM+αTNF), 30% CM obtained from IL-17A/F DKO Tc17 cells (DKO-CM) or 30% DKO-CM+ 5µg/ml anti-TNF antibodies (DKO-CM+αTNF) for 48h (mean ± s.d., n=3). Fold of mRNA expression is shown, normalised to the control (-), which was arbitrarily set to 1. (L) qPCR analysis for indicated gene expression by qPSC incubated with control medium (-), 50 ng/ml anti-IL-17A (IL-17A), 5ng/ml TNF (TNF), 50 ng/ml anti-IL-17A + 5 ng/ml TNF (IL-17A+TNF) (mean ± s.d., n=3). Fold of mRNA expression is shown, normalised to the control (-), which was arbitrarily set to 1. In (C-E,G,H,J-L) biological replicates are plotted. Bars show mean ± s.d, n=3. In (D,J,L) statistic was evaluated by one-way ANOVA followed by Dunnett's post hoc test *P<0.05, **P<0.01, ***P<0.001, ****P<0.0001, in (E,G,H) by two-tailed, unpaired *t*-test *P<0.05, ***P<0.001,***P<0.001, ****P<0.0001, in (L) **P*<0.05, ***P*<0.01, ***P<0.001, ****P<0.0001 by one-way ANOVA followed by Tukey's HSD multiple comparison test.

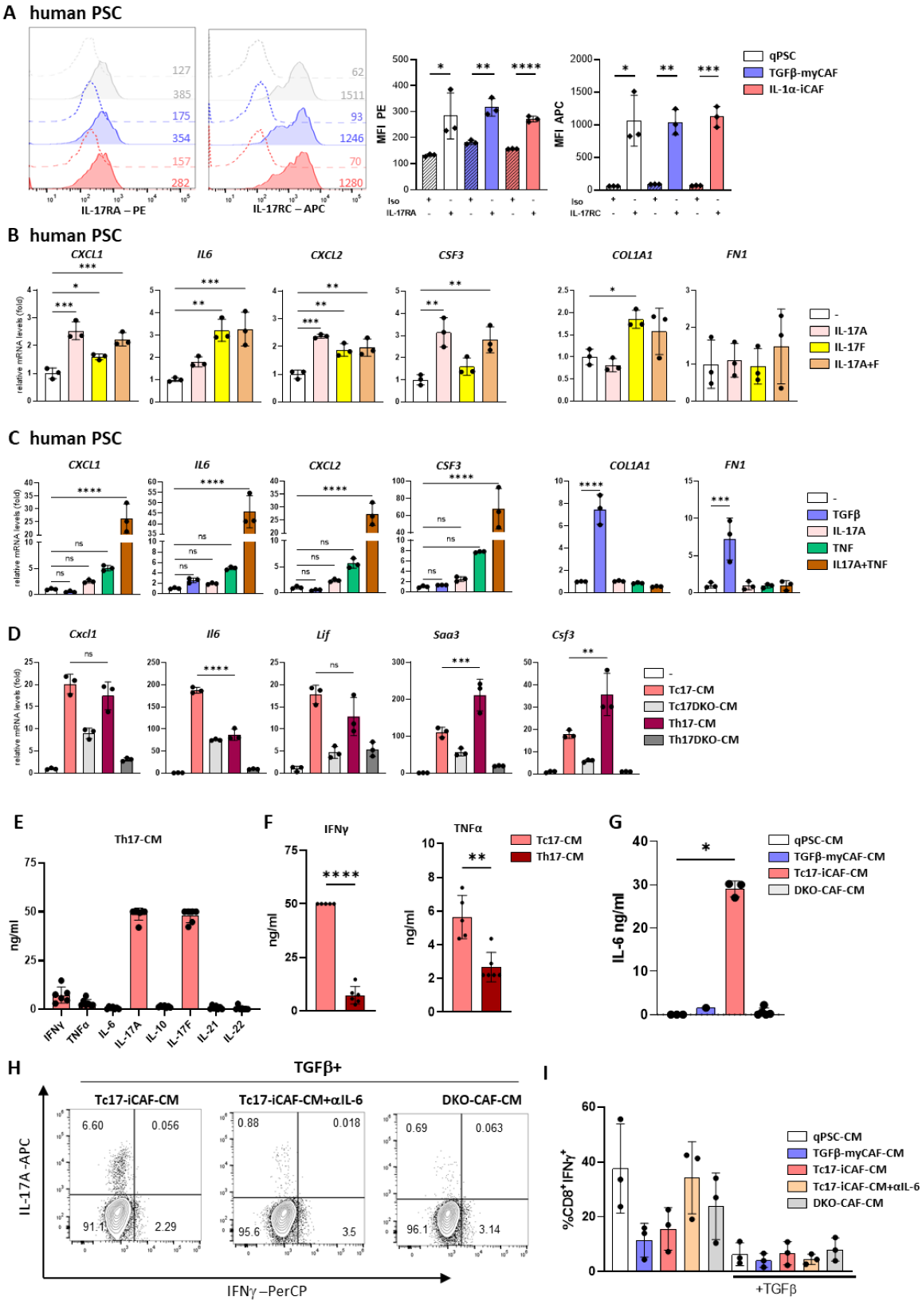
A human PSC
IL-17RA – PE
IL-17RC – APC
MFI PE
MFI APC
qPSC
TGFβ-myCAF
IL-1α-iCAF
B human PSC
CXCL1
IL6
CXCL2
CSF3
COL1A1
FN1
relative mRNA levels (fold)
IL-17A
IL-17F
IL-17A+F
C human PSC
TGFβ
TNF
IL17A+TNF
D
Cxcl1
Il6
Lif
Saa3
Csf3
Tc17-CM
Tc17DKO-CM
Th17-CM
Th17DKO-CM
E
Th17-CM
ng/ml
IFNγ
TNFα
IL-6
IL-17A
IL-10
IL-17F
IL-21
IL-22
F
IFNγ
TNFα
G
qPSC-CM
TGFβ-myCAF-CM
Tc17-iCAF-CM
DKO-CAF-CM
IL-6 ng/ml
H
TGFβ+
Tc17-iCAF-CM
Tc17-iCAF-CM+αIL-6
DKO-CAF-CM
IL-17A -APC
IFNγ –PerCP
I
%CD8+IFNγ+
+TGFβ

Supplementary Figure 5. IL-17A and TNF synergistically promote human iCAF differentiation. (A) FACS analysis of human PSC differentiated to qPSC, myCAF (induced from qPSC by addition of 5 ng/ml rhTGFβ to control medium for 48h) or IL-1α-iCAF (induced from qPSC by addition of 5 ng/ml rhIL-1α to control medium for 48h) for IL17RA and IL-17RC levels (n=3). (B,C) qPCR analysis for indicated gene expression by human qPSC incubated with control medium (-), 50 ng/ml rhIL-17A (IL-17A), 50 ng/ml rhIL-17F (IL-17F) or 50 ng/rh IL-17A + 50 ng/ml rhIL-17F (IL-17A+F) (n=3) (B) or with 2ng/ml rhTGFβ (TGFβ), 50 ng/ml IL-17A (IL-17A), 5 ng/ml rhTNF (TNF) or 50 ng/ml IL-17A + rhTNF (IL-17A+TNF) (n=3) (C) for 48h. Fold of mRNA expression is shown, normalised to the control (-), which was arbitrarily set to 1. (D) qPCR analysis for indicated marker expression by mouse qPSC incubated with control medium (-), 30% of Tc17-CM (Tc17-CM), 30% CM obtained from IL-17A/F DKO Tc17 cells (Tc17DKO-CM) 30% of Th17-CM (Th17-CM) or 30% CM obtained from IL-17A/F DKO Th17 cells (Th17DKO-CM) for 48h. Fold of mRNA expression is shown, normalised to the control (-), which was arbitrarily set to 1 (n=3). (E) Quantification of cytokines (ng/ml) produced by *in vitro* differentiated Th17 cells after restimulation with anti-CD3 antibodies for 24h (n=7). (F) Comparison of IFNγ and TNF secretion by Th17 vs Tc17 cells after restimulation with anti-CD3 antibodies for 24h (n=5-6). (G) ELISA for IL-6 from CM obtained from qPSC, TGFβ-myCAF, Tc17-iCAF and DKO-CAF after 48h of differentiation (n=3). (H,I) FACS analysis for frequency of $IFN\gamma^+$ and $IL\text{-}17A^+$ $CD8^+$ T cells differentiated in CM obtained from qPSC, myCAF, Tc17-iCAF, Tc17-iCAF + αIL-6 and DKO-CAF for 72 hours in the presence or absence of 2 ng/ml TGFβ after restimulation with PMA/Ionomycin for 4 h in the presence of brefeldin A (n=3). Left, representative FACS plots, right, quantification of the frequency of $CD8^+IFN\gamma^+$ cells is shown. In (A-G,I) biological replicates are plotted, bars show mean ± s.d. In (A,F) statistic were determined by two-tailed, unpaired *t*-test *P<0.05, **P<0.01, ***P<0.001, ****P<0.0001, in (B,C,D) by one-way ANOVA followed by Dunnett's post hoc test *P<0.05, **P<0.01, ***P<0.001, ****P<0.0001, ns (not significant), in (G) by Kruskal-Wallis-Test*P<0.05.

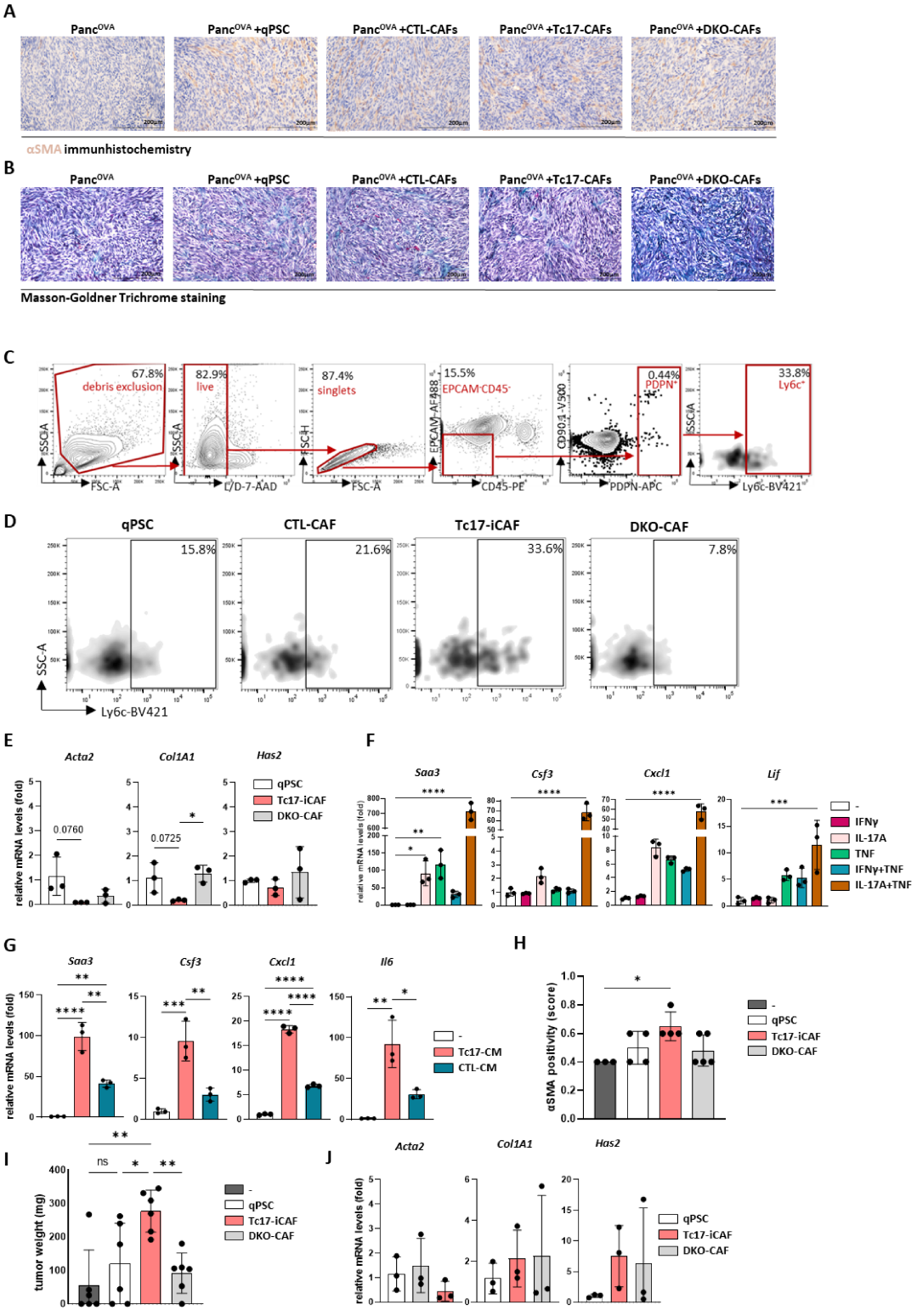

Supplementary Figure 6. Context-specific cytokine effects modulate PSC differentiation.

(A) αSMA staining performed on tumor tissue obtained from *Rag1*$^{-/-}$ mice, which were

subcutaneously co-injected with *in vitro* differentiated CD90.1$^+$qPSC, CD90.1$^+$CTL-CAF, CD90.1$^+$Tc17-iCAF or CD90.1$^+$DKO-iCAF and Panc^{OVA} tumor cells. The αSMA$^+$ cell quantification (brown staining) was performed based on previously published scoring[20]; scale bar 200 µm. (B) Masson-Goldner Trichrome staining to detect collagen (red spots) in tumor tissues; scale bar 200 µm. (C) Gating strategy for FACS analysis of subcutaneous murine tumor tissue samples. Acquired cells were first gated for debris exclusion (SSC-A vs FSC-A), followed by gating for living cells (L/D vs SSC-A) and then for single cells (FSC-H vs FSC-A). Fibroblasts were identified based on gating of CD45$^-$ and EPCAM$^-$ cells (EPCAM vs CD45, % of calculated EPCAM$^-$CD45$^-$ cells was based on the single-cell gate) and the expression of PDPN (PDPN vs CD90.1). In gated PDPN$^+$ cells Ly6c expression was determined (Ly6c vs SSC-A). (D) FACS analysis of Ly6c^{high} cell frequency in gated EPCAM$^-$CD45$^-$PDPN$^+$ fibroblasts in subcutaneous tumors of mice co-injected with qPSC, CTL-CAF, Tc17-iCAF or DKO-CAF. Representative FACS plots are shown. (E) qPCR analysis for indicated gene expression by EPCAM$^-$CD45$^-$PDPN$^+$CD90.1$^+$ cells sorted from subcutaneous Panc^{OVA} tumors of mice co-injected with qPSC, Tc17-iCAF and DKO-iCAF. Fold of mRNA expression is shown, normalised to qPSC group, which was arbitrarily set to 1 (n=3). (F) qPCR analysis for indicated gene expression by qPSC incubated with control medium (-), 50ng/ml IFNγ (IFNγ), 50 ng/ml IL-17A (IL-17A), 5 ng/ml TNF (TNF), 50ng/ml IFNγ + 5 ng/ml TNF (IFNγ+TNF) and 50 ng/ml IL-17A + 5 ng/ml TNF (IL-17A+TNF) for 48h. Fold of mRNA expression is shown, normalised to the control (-), which was arbitrarily set to 1 (n=3). (G) qPCR analysis for indicated gene expression by qPSC incubated with control medium (-), 30% of Tc17-CM (Tc17-CM) or 30% of CTL-CM (CTL-CM) for 48h. Fold of mRNA expression is shown, normalised to the control (-), which was arbitrarily set to 1 (n=3). (H) Quantification of αSMA staining in tumor tissue obtained from *Rag1*$^{-/-}$ mice (n=4-5) orthotopically injected with KPC cells alone (-) or together with qPSC (qPSC), Tc17-iCAF (Tc17-iCAF) or DKO-CAF (DKO-CAF) based on previously published scoring[20]. (I) Tumor weight of orthotopic tumors from *Rag1*$^{-/-}$ mice is shown (n=5-6 mice). (J) qPCR analysis for indicated gene expression by EPCAM$^-$CD45$^-$PDPN$^+$CD90.1$^+$ cells sorted from subcutaneous PaTu8988T tumors of mice co-injected with qPSC, Tc17-iCAF and DKO-CAF. Fold of mRNA expression is shown, normalised to qPSC group, which was arbitrarily set to 1 (n=3). (E-J) Biological replicates are plotted. Bars show mean ± s.d.. In (E,G,H,I,J) statistic was evaluated by one-way ANOVA followed by Tukey's HSD multiple comparison test *P<0.05, **P<0.01, ***P<0.001, ****P<0.0001, in (F) by one-way ANOVA followed by Dunnett's post hoc test *P<0.05, **P<0.01, ***P<0.001, ****P<0.0001.

A

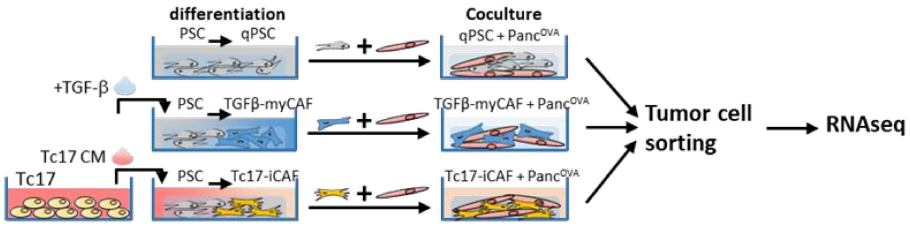
differentiation
PSC
qPSC
Coculture
qPSC + Panc^OVA
+TGF-β
PSC
TGFβ-myCAF
TGFβ-myCAF + Panc^OVA
Tc17 CM
Tc17
PSC
Tc17-iCAF
Tc17-iCAF + Panc^OVA
Tumor cell sorting
RNAseq

B

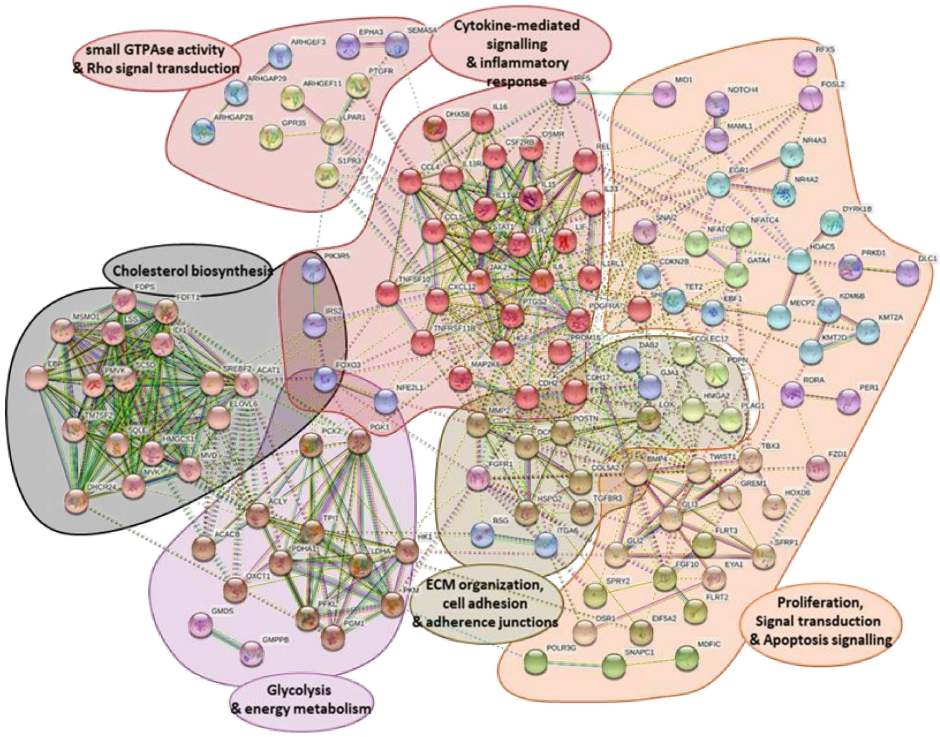
small GTPAse activity & Rho signal transduction
Cytokine-mediated signalling & inflammatory response
Cholesterol biosynthesis
ECM organization, cell adhesion & adherence junctions
Proliferation, Signal transduction & Apoptosis signalling
Glycolysis & energy metabolism

C

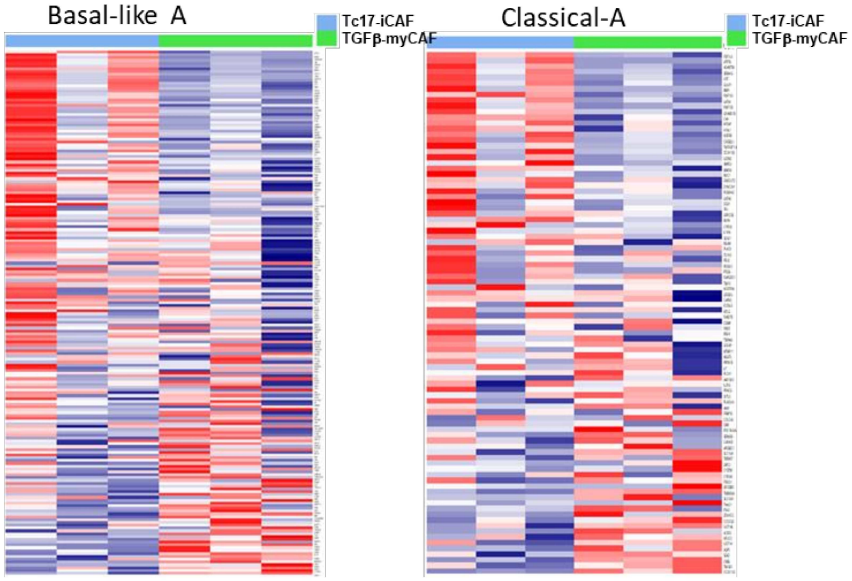
Basal-like A
Tc17-iCAF
TGFβ-myCAF
Classical-A
Tc17-iCAF
TGFβ-myCAF

Supplementary Figure 7. Transcriptional signatures of tumor cells after co-culture with Tc17-iCAF vs TGFβ-myCAF. (A) Scheme of the experimental design showing RNA-sequencing of sorted $Panc^{OVA}$ tumor cells after matrigel embedded co-culture with qPSC, TGFβ-myCAF or Tc17-iCAF. (B) STRING protein expression mapping of significantly upregulated genes in $Panc^{OVA}$ cells (FDR<0.1) after co-culture with Tc17-iCAF. Only experimentally verified (confidence level 0.4) interactions between query proteins are shown. The distance between genes and the orientation is random. Highlighted are protein networks corresponding to the identified GO pathways in gene modules 3-7 in Figure 5B. (C) Heatmaps of color-coded z-scores from the rlog transformed expression values based on the GSEA for differential expression of Basal-like A or Classical-A human PDAC transcripts[18] in $Panc^{OVA}$ cells after 36 h coculture with Tc17-iCAF vs TGFβ-myCAF.

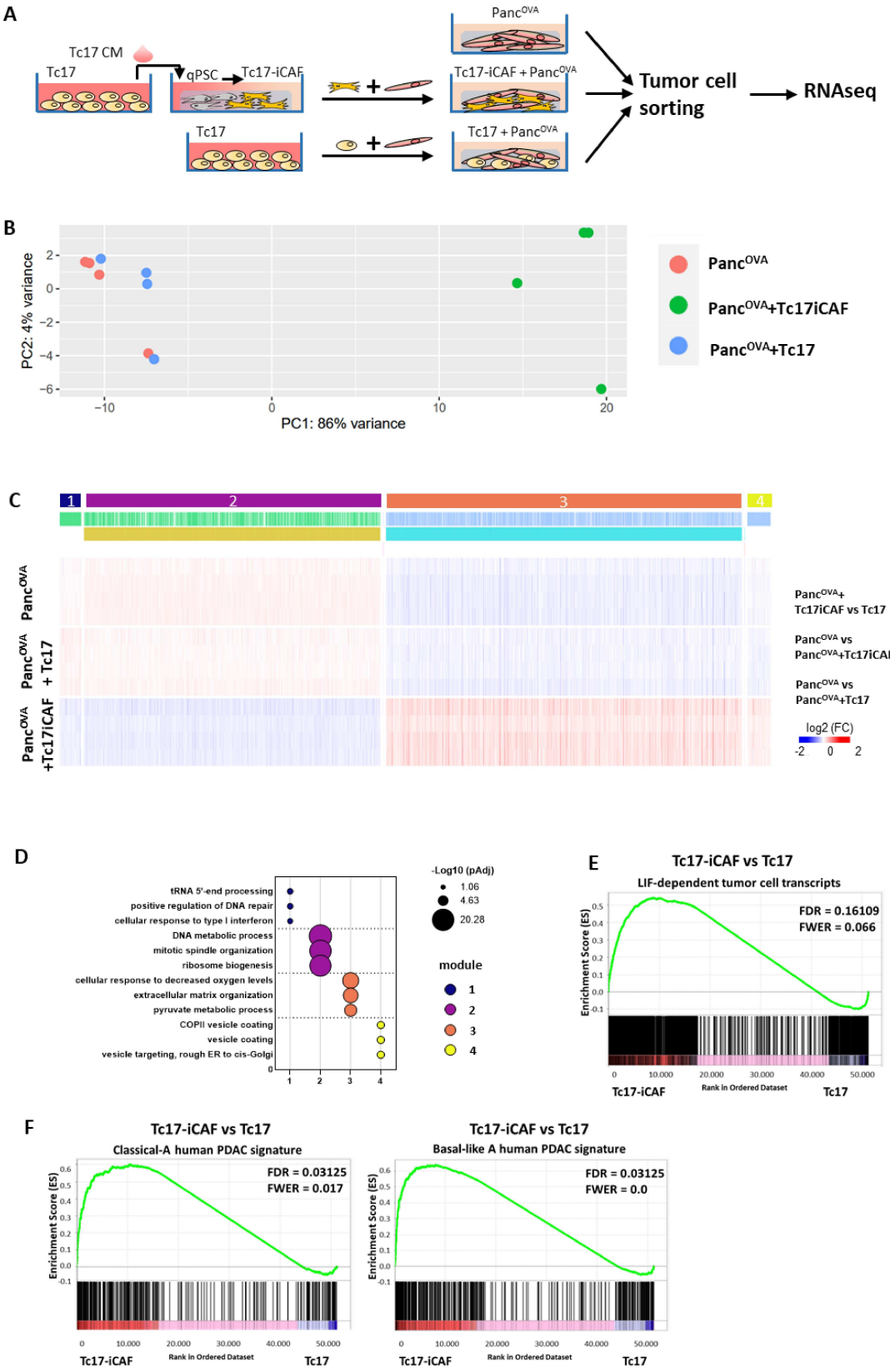
A
Tc17 CM
Tc17
qPSC
Tc17-iCAF
Tc17
PancOVA
Tc17-iCAF + PancOVA
Tc17 + PancOVA
Tumor cell sorting
RNAseq
B
PC2: 4% variance
PC1: 86% variance
PancOVA
PancOVA+Tc17iCAF
PancOVA+Tc17
C
PancOVA
PancOVA + Tc17
PancOVA +Tc17iCAF
PancOVA+ Tc17iCAF vs Tc17
PancOVA vs PancOVA+Tc17iCAF
PancOVA vs PancOVA+Tc17
down up
log2 (FC)
D
tRNA 5'-end processing
positive regulation of DNA repair
cellular response to type I interferon
DNA metabolic process
mitotic spindle organization
ribosome biogenesis
cellular response to decreased oxygen levels
extracellular matrix organization
pyruvate metabolic process
COPII vesicle coating
vesicle coating
vesicle targeting, rough ER to cis-Golgi
-Log10 (pAdj)
1.06
4.63
20.28
module
E
Tc17-iCAF vs Tc17
LIF-dependent tumor cell transcripts
FDR = 0.16109
FWER = 0.066
Enrichment Score (ES)
Rank in Ordered Dataset
Tc17-iCAF
Tc17
F
Tc17-iCAF vs Tc17
Classical-A human PDAC signature
FDR = 0.03125
FWER = 0.017
Tc17-iCAF vs Tc17
Basal-like A human PDAC signature
FDR = 0.03125
FWER = 0.0

Supplementary Figure 8. Transcriptional signatures of tumor cells after co-culture with Tc17 cells vs Tc17-iCAF. (A) Scheme of the experimental design showing RNA-sequencing of sorted Panc^{OVA} tumor cells after matrigel embedded co-culture with Tc17-iCAF or Tc17 cells for 36h. (B) Principal component analysis (PCA) of the top 500 genes with highest row variance expressed by Panc^{OVA} cells cultured alone (red) or co-cultured with Tc17-iCAF (green) or with Tc17 cells (blue). (C) Heatmap of differentially expressed genes (Z score normalized, FDR≤0.001) by Panc^{OVA} cells after 36h of co-culture with Tc17 cells or Tc17-iCAF classified into modules based on the mutual up- or down-regulation (n=4, biological replicates). (D) Pathway enrichment analysis for Gene Ontologies (GO): Biological processes. Bubble graph displays the three significantly enriched pathways by –log10 value (p adj) for four modules established in (C). (E) GSEA for differential expression of LIF-dependent pancreatic cancer cell transcripts obtained from *Lifr^{WT} KP$^{f/f}$CL* vs *Lifr$^{f/f}$KP$^{f/f}$CL* mice[17] in Panc^{OVA} tumor cells ± Tc17-iCAF co-culture. (F) GSEA for differential expression of Classical-A or Basal-like A human PDAC transcripts[18] in Panc^{OVA} tumor cells ± Tc17-iCAF co-culture.

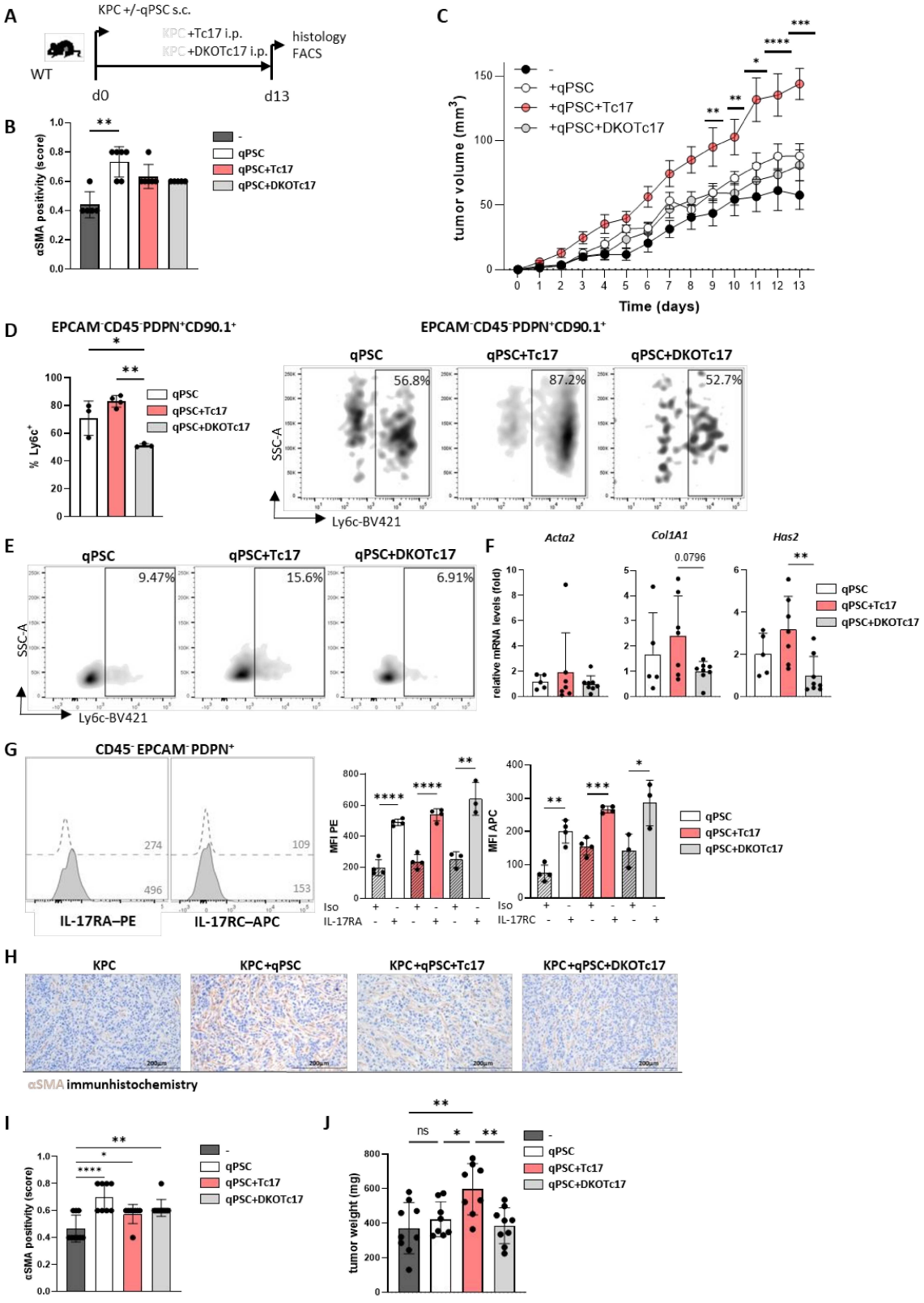
A
KPC +/-qPSC s.c.
KPC +Tc17 i.p.
KPC +DKOTc17 i.p.
histology
FACS
WT
d0
d13
B
αSMA positivity (score)
-
qPSC
qPSC+Tc17
qPSC+DKOTc17
C
tumor volume (mm3)
Time (days)
D
EPCAM-CD45-PDPN+CD90.1+
% Ly6c+
qPSC
qPSC+Tc17
qPSC+DKOTc17
56.8%
87.2%
52.7%
SSC-A
Ly6c-BV421
E
9.47%
15.6%
6.91%
F
Acta2
Col1A1
Has2
0.0796
relative mRNA levels (fold)
G
CD45-EPCAM-PDPN+
274
496
109
153
IL-17RA–PE
IL-17RC–APC
MFI PE
MFI APC
Iso
IL-17RA
IL-17RC
H
KPC
KPC+qPSC
KPC+qPSC+Tc17
KPC+qPSC+DKOTc17
αSMA immunhistochemistry
I
αSMA positivity (score)
J
tumor weight (mg)
ns

Supplementary Figure 9. Tc17 cells promote pancreatic tumor growth *in vivo*. (A) Scheme of the experimental design. 5×10^5 KPC tumor cells ± 5×10^5 CD90.1$^+$qPSC were subcutaneously co-injected into WT mice, which on the same day received i.p. injections of PBS or 10^6 WT (Tc17) or IL-17A/FDKO Tc17 (DKOTc17) cells. Histology and FACS analysis were performed at the indicated end of the experiment. (B) Quantification of αSMA staining in tumor tissue of mice injected with KPC cells alone (-) or co-injected with qPSC (qPSC), with qPSC +Tc17 cells (qPSC+Tc17) or with qPSC + DKOTc17 cells (qPSC+DKOTc17), based on previously published scoring[20], (mean ± s.d., n=5-6). (C) Tumor growth curve of subcutaneous KPC tumors is shown (mean ± sem, n=6-8 mice). *P<0.05, **P<0.01, ***P<0.001, ****P<0.0001 indicate the tumor volume comparisons between the groups qPSC+Tc17 vs qPSC. (D) FACS analysis of Ly6c^{high} cell frequency in gated EPCAM$^-$CD45$^-$PDPN$^+$CD90.1$^+$ fibroblasts in subcutaneous KPC tumors after injection of PBS, Tc17 or DKOTc17 cells (mean ± s.d., n=3 tumors). Left, quantification of the frequency of Ly6c^{high} EPCAM$^-$CD45$^-$PDPN$^+$ cells, right, representative FACS plots are shown. (E) FACS analysis of Ly6c^{high} cell frequency in gated EPCAM$^-$CD45$^-$PDPN$^+$ cells in subcutaneous Panc^{OVA} tumors after injection of PBS, Tc17 or DKOTc17. Representative FACS plots are shown. (F) qPCR analysis for indicated gene expression by sorted EPCAM$^-$CD45$^-$PDPN$^+$ cells obtained from subcutaneous Panc^{OVA} tumors after injections as indicated (mean ± s.d., n=5-8). Fold mRNA expression is shown, normalised to the DKOTc17 group, which was arbitrarily set to 1. (G) FACS analysis of EPCAM$^-$CD45$^-$PDPN$^+$ fibroblasts in subcutaneous Panc^{OVA} tumors for IL17RA and IL-17RC levels. Left, representative histograms of IL-17RA and IL-17RC levels expressed by EPCAM$^-$CD45$^-$PDPN$^+$ fibroblasts in subcutaneous Panc^{OVA} tumors after co-injection of qPSC, dashed line indicates isotype control. Right, quantification of IL-17RA and IL-17RC levels expressed by gated EPCAM$^-$CD45$^-$PDPN$^+$ fibroblasts in subcutaneous Panc^{OVA} tumors after injections as indicated (mean ± s.d., n=3-4 tumors). (H) αSMA staining in tumor tissue from WT mice, which were orthotopically injected with KPC tumor cells and ± CD90.1$^+$qPSC, followed by intraperitoneal adoptive transfer of WT (Tc17) or DKO Tc17 (DKOTc17) cells. The αSMA$^+$ cell quantification (brown staining) was performed based on previously published scoring[20]; scale bar 200 µm. (I) Quantification of αSMA staining in tumor tissue of WT mice (mean ± s.d., n=8-9) orthotopically injected as indicated based on previously published scoring[20]. (J) Tumor weight of orthotopic tumors in WT mice is shown (tumor volume in mm^3; mean ± sd, n=8-9 mice). (B,D,F,G,I,J) biological replicates are plotted. In (B) statistics was evaluated by Kruskal-Wallis-Test, **P<0.01, in (C) by two-way ANOVA followed by Bonferroni post-hoc test *P<0.05, **P<0.01, ***P<0.001, ****P<0.0001, in (D,J) by one-way ANOVA followed by Tukey's HSD multiple comparison test, *P<0.05, **P<0.01, ***P<0.001, in (F,I) by one-way ANOVA followed by Dunnett's post hoc test, *P<0.05, **P<0.01, ****P<0.0001, in (G) two-tailed, unpaired *t*-test, *P<0.05, **P<0.01, ***P<0.001, ****P<0.0001.

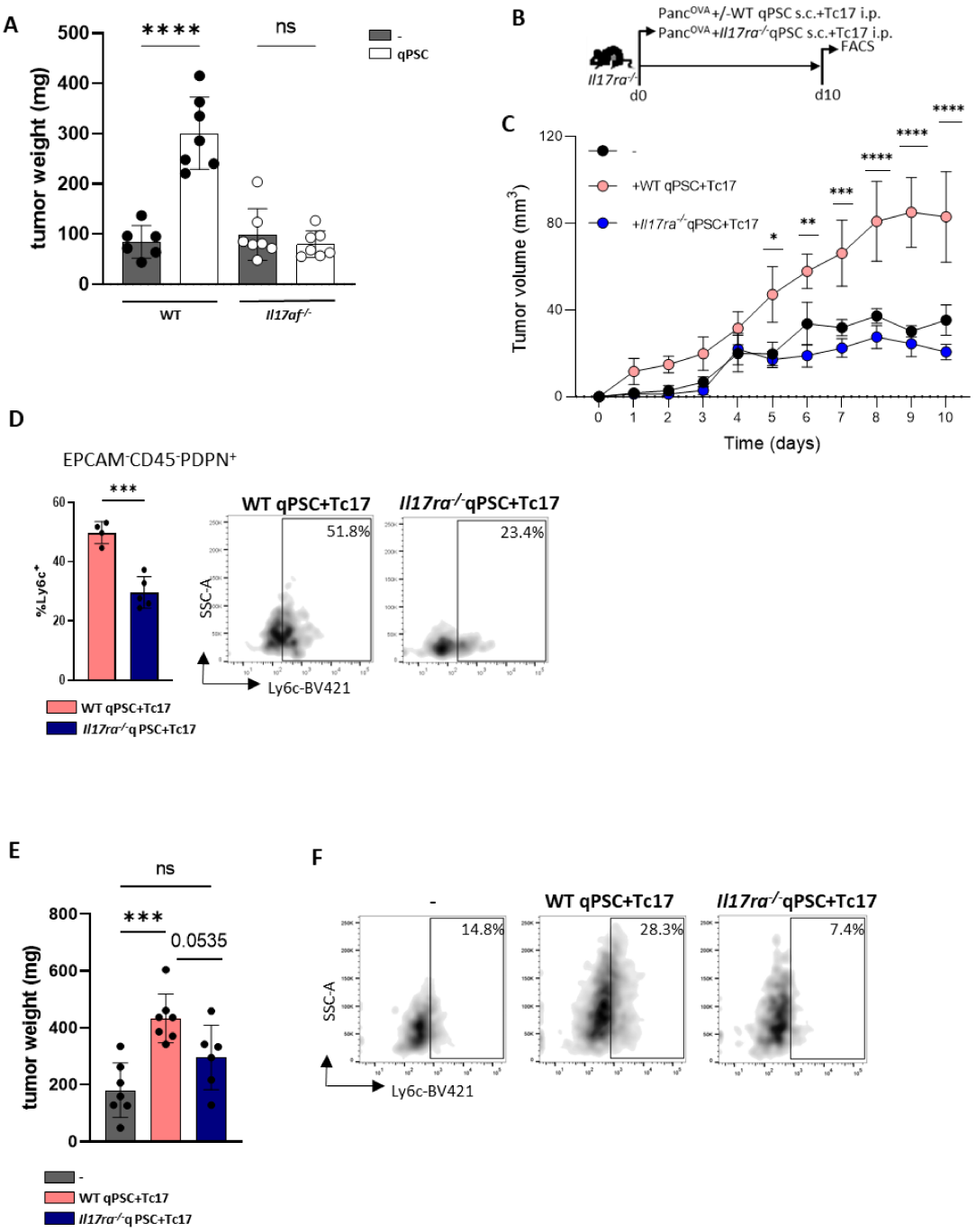

Supplementary Figure 10. IL-17RA expressed by PSC is required for Tc17-driven tumor growth *in vivo*. (A) Tumor weight of orthotopic tumors from WT vs *Il17a/f*$^{-/-}$ mice is shown (tumor weight in mg; mean ± sd, n=6-7 mice). (B) Scheme of the experimental design. 5×10^5 Panc^{OVA} tumor cells with/without 5×10^5 WT or *Il17ra*$^{-/-}$CD90$^+$qPSC were subcutaneously injected into *Il17ra*$^{-/-}$ mice, which at the same received i.p. injections of PBS or 10^6 Tc17 cells or PBS. The CAF analysis was performed at the indicated end of the experiment. (C) Tumor

growth curve of subcutaneous tumors of mice injected with $Panc^{OVA}$ cells alone (-) or co-injected with WT qPSC + Tc17 cells (WT qPSC+Tc17) or with *Il17ra*$^{-/-}$ qPSC + Tc17 cells (*Il17ra*$^{-/-}$ qPSC+Tc17) (mean ± sem, n=4-6 mice). **P*<0.05, ***P*<0.01, ****P*<0.001, *****P*<0.0001 indicate the tumor volume comparisons between the groups WT qPSC+Tc17 vs *Il17ra*$^{-/-}$ qPSC+Tc17. (D) FACS analysis of $Ly6c^{high}$ cell frequency in gated $EPCAM^{-}CD45^{-}PDPN^{+}$ fibroblasts in subcutaneous $Panc^{OVA}$ tumors of *Il17ra*$^{-/-}$ mice treated as indicated. (mean ± s.d., n=5). Left, quantification of the frequency of $Ly6c^{high}$ $EPCAM^{-}CD45^{-}PDPN^{+}$ cells. Right, representative FACS plots are shown. (E) Tumor weight of orthotopic tumors from *Il17ra*$^{-/-}$ mice is shown (tumor volume in mm^3; mean ± sd, n=6-7 mice). (F) Representative FACS plots of $Ly6c^{high}$ cell frequency in gated $EPCAM^{-}CD45^{-}PDPN^{+}$ fibroblasts in orthotopic KPC tumors of *Il17ra*$^{-/-}$ mice treated as indicated. (A, C-E) the results from individual mice are plotted. In (A,E) ****P*<0.001, *****P*<0.0001 and *P* values by one-way ANOVA followed by Tukey's HSD multiple comparison test, in (C) **P*<0.05, ***P*<0.01, ****P*<0.001, *****P*<0.0001 determined by two-way ANOVA with Bonferroni post-hoc test, in in (D) two-tailed, ****P*<0.001 by unpaired *t*-test.